JKAU: Earth Sci., **Vol. 17,** pp: 117-153 (2006 A.D. / 1427 A.H.)

Geology and Geochemistry of Jabal Ghadarah Ophiolitic Mélange, Zalim Quadrangle, Central Saudi Arabia

H.A. Harbi, A.A. Eldougdoug and N.S. Al Jahdli*

Faculty of Earth Sciences, King Abdulaziz University, and
**Saudi Geological Survey, Jeddah, Saudi Arabia*

Received: 5/3/2006 Accepted: 28/5/2006

Abstract. The Precambrian rocks encountered at Jabal Ghadarah area can be grouped into: metaultramafites, arc metavolcanosedimetary rocks, syn- to late-orogenic granitoids, intramontane molasse-type sediments and post-orogenic monzogranite. At Jabal Ghadarah, the meta-ultramafic rocks and associated listvenites are mainly exposed along a NNE trending thrust fault dipping to the east, in contact with the arc metavolcanosedimentary rocks. The metaultramafites are characterized by the presence of numerous fragments of variable sizes (metagabbros, metabasalts, schists, amphibolites and marble). Major and trace elements distribution indicates that the metagabbros, metabasalts and amphibolites are tholeiitic in character and of ocean floor affiliation. The amphibolites were derived either from mafic or ultramafic protoliths. Chromite from the serpentinite and listvenite show a wide range of major oxides contents comparable to Alpine-type chromite. The metaultramafites and associated rock fragments are interpreted as an ophiolitic mélange imbricated with the arc metavolcanosedimentary sequence during accretion of the Arabian shield, contrary to the intrusive nature suggested by earlier workers.

Introduction

Previous Studies – Regional

The area of Zalim quadrangle has been studied by many workers, because it is known for the presence of great number of gold occurrences including Zalim mine, which was operated for a short period in early 1950's and rapidly closed

after a very limited production. The area witnessed numerous exploration activities during the nineties of the last century. Currently numerous prospects are under exploration activities by Ma'aden company and two promising gold-bearing listvenite prospects, namely Al Mansura and El Messara, were defined along Bir Tawila thrust.

Also the geology of the quadrangle drew the attention of many workers because of its location on the Nabitah suture zone (Agar, 1984a and Viland, 1986). Understanding the geology of this part of the shield helps greatly in interpreting its evolution.

The area of the present study occupies the north central part of Zalim quadrangle and is located in the central eastern edge of the Nabitah suture zone and orogenic belt (Fig. 1). The Nabitah orogenic belt defines a 100-200 km wide zone of crustal deformation, remobilization and plutonism along the margins of the Asir, Hijaz, and Afif terranes (Schmidt *et al.*, 1979 & Stoeser and Camp, 1984). The belt consists of broad, linear complexes of synorogenic unfoliated to gneissic granitoid plutonic rocks, separated by regions of middle greenschist to amphibolite-grade metamorphic rocks (Stoeser and Camp, *op. cit*.). The southern and central part of the orogenic belt contains a north-trending linear belt of ultramafic and mafic rocks (Fig. 1), which was interpreted by Frisch and Al Shanti (1977) as being an ophiolitic complex along a suture zone between two juxtaposed arcs. Schmidt *et al.*, (*op. cit.*) supported this interpretation and referred to this zone as Nabitah suture (Fig. 1). They described the major tectonic features of the belt and interpreted them as representing a major episode of westward-directed nappe formation and crustal upturning related to collision between the western part of the shield and a continental block to the east (Ar Rayn Plate).

Stoeser and Camp (1984) defined the Nabitah orogenic (or mobile) belt and interpreted the suture zone and belt as marking the site of collision between the Afif terrane and the western arc terranes. They showed by U/Pb zircon dating that the synorogenic plutonism within the southern part of the belt occurred between 680 and 640 Ma. The western part of the belt developed within the western arc terranes and incorporated much of the Tarib arc assemblages of the Asir terrane in the south and Hijaz arc assemblage of the Hijaz terrane in the north (Fig. 1). Similarly, the eastern part of the belt is superimposed over the continental margin of the Afif terrane in the north and over a continental margin similar to the Ar Rayn terrane in the south.

During the last two decades, the great similarity in both structural fabric elements and composition between the on-land ophiolites and the present day oceanic lithosphere was detected by many workers (*e.g.* Gass, 1968; Dewey and Bird, 1971; Christensen and Salisbury, 1975 & Gass and Smewing, 1981). Such similarity led to the conclusion that these ophiolites are essentially allochthon-

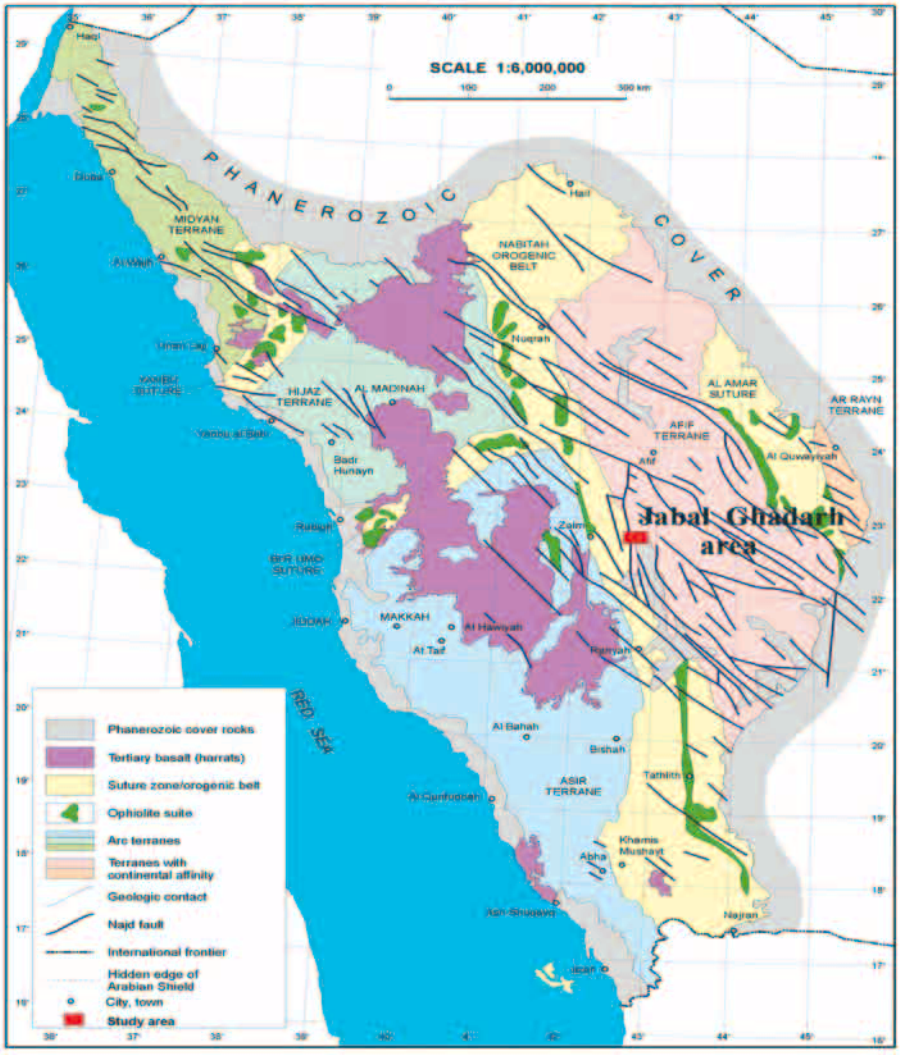

Fig. 1. Tectonic sketch map of the Arabian Shield showing terranes and suture zones (modified after Stoeser and Camp, 1984).

ous fragments of oceanic crust and upper mantle (*e.g.* Coleman, 1971 and 1977; Church, 1972; Hutchinson; 1975 and Gass, 1981). However, the mechanism of tectonic emplacement of ophiolites into continental margins is still a subject of controversy. According to Gansser (1974) an ophiolitic mélange is defined as an olistostromal and tectonic mixture of ophiolitic material and sediments of oceanic origin with exotic blocks, reflecting areas, which have subsequently disappeared. In the present study the term ophiolitic mélange as given by Gansser (*op. cit.*) is adopted in a descriptive sense.

Ophiolitic mélange has been described from different parts of the Arabian Shield, *e.g.*, Al Amar-Idsas belt, Jabal Humayyan-Jabal Sabhah belt, Al Bijadiyah-Halaban belt, Hulayfah-Hamdah-Nabitah belt, Jabal Ess-Jabal Al Wask belt and Bir Umq-Jabal Thurwah belt (Bakor *et al*., 1976; Stoeser and Camp, 1984; Al Shanti, 1993; El-Mahdy and Al Shanti, 2001 & Al Shanti and El-Mahdy, 2001; Al-Saleh and Boyle, 2001) (Fig. 1) and the Nubian Shield (El Sharkawy and El Bayoumi, 1979; Shackleton *et al.*, 1980; Basta, 1983; Abdel Wahed, 1985; Kroner, 1985; Abdel Wahed *et al*., 1986; Takla *et al*., 1990 & Johnson *et al.*, 2003).

Amphibolites have been described as a common component of the ophiolitic mélange *e.g.* Oman (Lippard *et al.*, 1986), Newfoundland (Williams and Smythe, 1973), Haimour, Eastern Desert Egypt (Abd El-Naby, *et al.*, 2000), Alaska (Harris, 1987), Southern Tibet (Huot *et al.*, 2002), Northwest Syria (Al-Riyami *et al*., 2002) as well as the amphibolites associated with ophiolitic belts in the Arabian Shield (Letalenet, 1979, Worl and Elsass, 1980; Kemp *et al*., 1982 & Le Metour *et al*., 1983).

Previous Work on the Study Area

The study area is covered mainly by a group of metavolcanosedimentry rocks and metasediments, which were intruded by a group of granitoid rocks. The Bir Tawilah thrust runs nearly N-S at the center of the area and is decorated by numerous bodies of ultramafic rocks altered to listvenite (Fig. 2).

Feybesse and LeBel (1984) described the rocks east of the Bir Tawilah thrust as micaceous fine-grained schists of the As Siham formation, while the Bani Ghayy group metasediments, which consist of conglomerate, greywacke and sandstone and located west of the listvenite was described as Murdamah group.

During geological and mineral exploration studies of Siham-As Suq belt, Elsass and Vaillant (1983) described the Bir Tawilah gold mineralization as being associated with quartz and listvenite, occurring along a major thrust fault.

Agar (1984b and 1985) studied the succession of the Bani Ghayy group metasediments west of the Jabal Ghadarah-Bir Tawilah thrust and mentioned that the

Bani Ghayy group was deposited in elongated grabens filled with sedimentary rocks of the Bani Ghayy group (conglomerates, greywackes, and limestones, with subordinate siltstones). The Bani Ghayy group is associated with bimodal volcanics and the presence of deformed ultramafic rocks within internal faults, which suggest that the grabens were floored, in part, by primitive mantle-derived crust. Agar (1984b and 1985) considered the sediments east of the Bir Tawilah thrust belong to Siham group.

Labbé (1984) carried out mineral exploration studies in the Bir Tawilah district, and found that the gold in the wadi alluvial sediments near Jabal Ghadarah, was derived from a hill 1800m long and 150m wide, and is associated with quartz veins in listvenitized ultramafic rocks. Nineteen alluvial samples were collected from the wadis, which drain Jabal Ghadarah. Fourteen samples of them displayed gold grains.

Labbé (1984) described the Jabal Ghadarah pluton as medium-grained quartz leucodiorite rich in pyrite, which intrudes the Murdamah group rocks to the west of the listvenite. This pluton appears to post-date the overthrust and is not affected by the north-south schistosity parallel to the fault which affected the Murdamah group rocks. Labbé (*op. cit.*) mentioned that the "... Bir Tawilah thrust fault is injected by a strip of mainly ultrmafic rocks (dunite) metamorphosed and altered to serpentinite, chlorite serpentine schist. Commonly such rocks were subsequently transformed to listvenites ...". Labbé (*op. cit.*) described two types of listvenite from Bir Tawilah thrust fault: 1) Banded silicified listvenite, which represents the magnesian pole (about 30% MgO) and 2) Red ferruginous listvenite that represents the calcic pole (about 36% CaO).

Viland (1986) classified the volcanosedimentary rocks into early Hulyfah (to the east of the Bir Tawilah thrust), and late Hulyfah (west of the Bir Tawilah thrust), and were described as flysch-type sediments deposited in a forearc environment. These volcanosedimentary rocks were intruded by several granitoid plutons. The metasedimentry rocks exposed at Jabal Bani Ghayy were considered as a separate unit, (Murdamah group molasse-type sediments), which is younger than Hulyfah volcanosedimentary rocks.

Billa (1987) carried out mineral exploration at Jabal Al Ghadhara and mentioned that the Jabal Ghadarah gold prospect is hosted by a small granodiorite intrusion of late proterozoic age along the contact between the proterozoic metasedimentary rocks and the carbonatized ultramafic rocks (listvenite). A surface investigation and percussion drilling totalling 1227m have defined an ore body with indicated reserves of at least 330,000 tons of ore grading 3.2 g/t Au. Billa (*op. cit.*) described mafic volcanic rocks at the contact between ultramafic and metasediments and considered them to represent volcanic activity associated with the ultramafic intrusion.

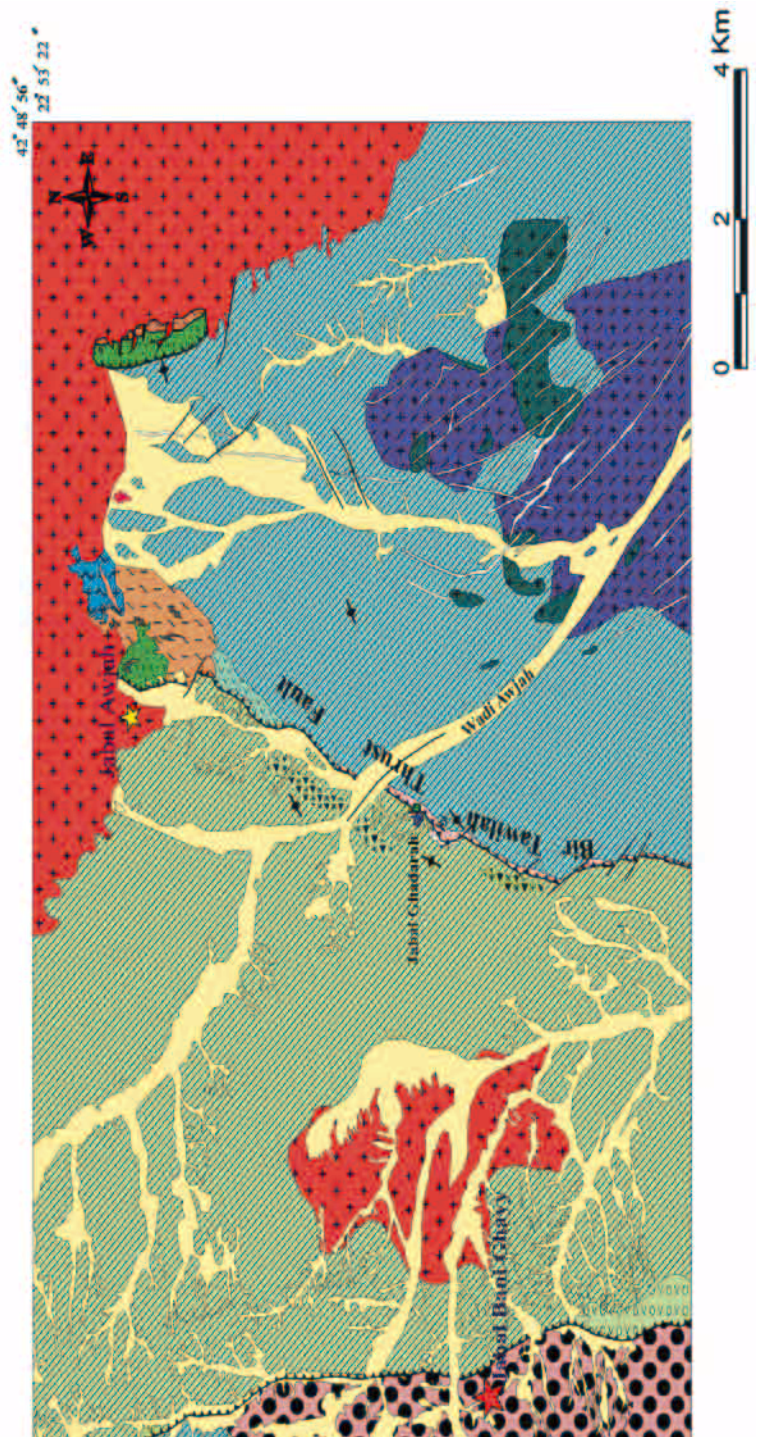

Fig. 2. Photogeological map of Jabal Ghadarah area (After Al Jahdli, 2004).

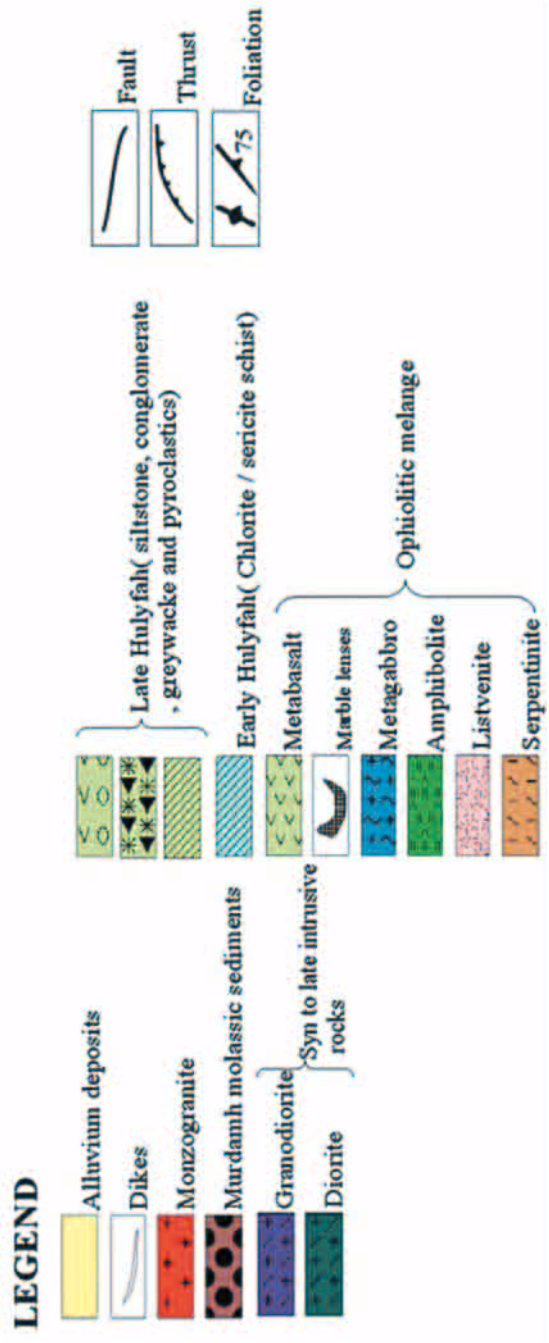
LEGEND
Alluvium deposits
Dikes
Monzogranite
Murdamh molassic sediments
Granodiorite
Diorite
Syn to late intrusive rocks
Late Hulyfah(siltstone, conglomerate , greywacke and pyroclastics)
Early Hulyfah(Chlorite / sericite schist)
Metabasalt
Marble lenses
Metagabbro
Amphibolite
Listvenite
Serpentinite
Ophiolitic melange
Fault
Thrust
Foliation
75

Fig. 2. Contd.

The geology of Zalim quadrangle was studied by Agar (1988) and reported that the Jabal Ghthylib (Ghadarah) is associated with Au-Ag mineralization which is hosted by granodiorite pluton. The listvenite in Bir Tawilah district was described as fault gouges material (deformed ultramafic rocks) and contains anomalous values of nickel and chromium and pods of serpentinite.

The metasediments to the east of Jabal Ghadarah-Bir Tawilah thrust was described by Agar (*op. cit*.) as Nawm Formation, which belongs to the Siham group (volcanic arc). The Nawm formation consists of basalt, andesite, shale, tuffaceous sandstone, siltstone and marble with minor amount of ultramafic bodies, which occur as sills.

Aim of the Study and Methods

The aim of the present study is to characterize the ultramafic rocks and associated rock fragments petrographically and chemically in order to define their tectonic setting.

The chemical analysis were carried out at Saudi Geological Survey, Jeddah. The major oxides were analyzed by atomic absorption, while the trace elements were determined by ICP techniques (Perken-Elmer Model 2000). For chromite analysis, SEM-EDX (Philips Model XL30) house at the Central laboratories of the Egyptian Geological Survey, Cairo was used at 40 kV accelerating voltage and a resolution for w. (3.5 nμ).

Field Relations and Petrography

The term ophiolitic mélange is introduced for the first time to describe the geology of the study area. The ophiolitic mélange consists of ultramafic rocks (serpentinites and listvenite), metagabbros, metabasalts, marble lenses and amphibolites. The ophiolitic mélange occupies the hanging wall of the major Bir Tawilah thrust fault. The footwall is represented by the late Hulyfah volcanosedimentary rocks. The listvenite zone along the Bir Tawilah major thrust fault marks the contact between the late Hulyfah volcanosedimentary rocks and the ophiolitic mélange (Fig. 2). These serpentinites have been considered as intrusive by Agar (1984a & b and 1988) and Billa (1987).

Ultramafic Rocks

The ultramafic rocks are common and, represented by serpentenites and listvenites. They are irregular in distribution and size, from mountains (such as Jabal Ghadarah) to vast flat areas with small blocks of outcrops, especially at the north central part of the study area. Also, the ultramafic rocks occur in the north eastern part closer to the contact with the younger granite of Awjah com-

plex. The sheared serpentenites are supposed to be the matrix of the ophiolitic mélange.

The serpentenites are sheared and best exposed in the north central part (Fig. 2). They occur as large flat or small unmappable outcrops. The serpentinites are green to dark green, brownish to yellowish in color and sometime exhibit mesh texture. Magnesite occurs as veinlets along the joint planes and fractures in the serpentenites. Microscopically, the serpentinites are sheared, banded and composed of antigorite, lizardite, bastite, talc and accessory opaques (Plate 1a).

The listvenites of Bir Tawilah area extend for more than 12 km along the Bir Tawilah thrust fault which is dipping to the east. The listvenites and related rocks are between 1-300 m thick in the outcrop. The best outcrop is represented by Jabal Ghadarah, which consists of a group of hills oriented north-northeast/ south-southwest and rising about 40 m above the surrounding area (Plate 1b).

The listvenite contains fragments of mafic and ultramafic rocks (Plate 1c). These fragments range from 2 to10 m across. The Bir Tawilah listvenite is affected by the Najd left lateral strike-slip faults striking N30º-50ºW (Fig. 2). The listvenite at Jabal Ghadarah occurs as massive to highly fractured blocks. The fresh listvenite is greenish gray in color and contains fresh disseminated sulphides, green fuchsite and disseminated chromite and magnetite in addition to carbonate (Plate 1d). Upon weathering listvenites are gradually altered to brownish to reddish brown colored rocks (Plate 1e).

Metamorphosed serpentinites and listvenites were found near the contact with the Awja monzogranite intrusion, and are characterized by the association of olivine, talc, tremolite, magnesite and dolomite (Plate 1f and Plate 2a). Such assemblage is characteristic to amphibolite hornfels facies. Similar assemblages have been described from metamorphosed serpentenites from Canada (Paktunc, 1984). These rocks can be classified into: 1) Talc tremolite metaserpentinites and 2) Talc lizardite listvenite.

The talc tremolite metaserpentinites are found at the northeastern sector of the study area. They are brownish to yellowish in color, sheared and form flat unmappable outcrops. The metaserpentinites are associated with amphibolites adjacent to the Awja monzogranitic intrusion. These rocks have been formed by thermal metamorphism of serpentinites as evident from the presence of minor serpentine minerals and chromite.

The talc lizardite listvenite is recorded in the north central part of the study area where listvenite is present in contact with the Awja monzogranite. They are fine grained brownish to yellowish and massive to slightly foliated. The rocks consist of serpentine minerals (lizardite), carbonate (magnesite), talc and accessory opaques (Plate 2b and c). The opaque minerals are represented main-

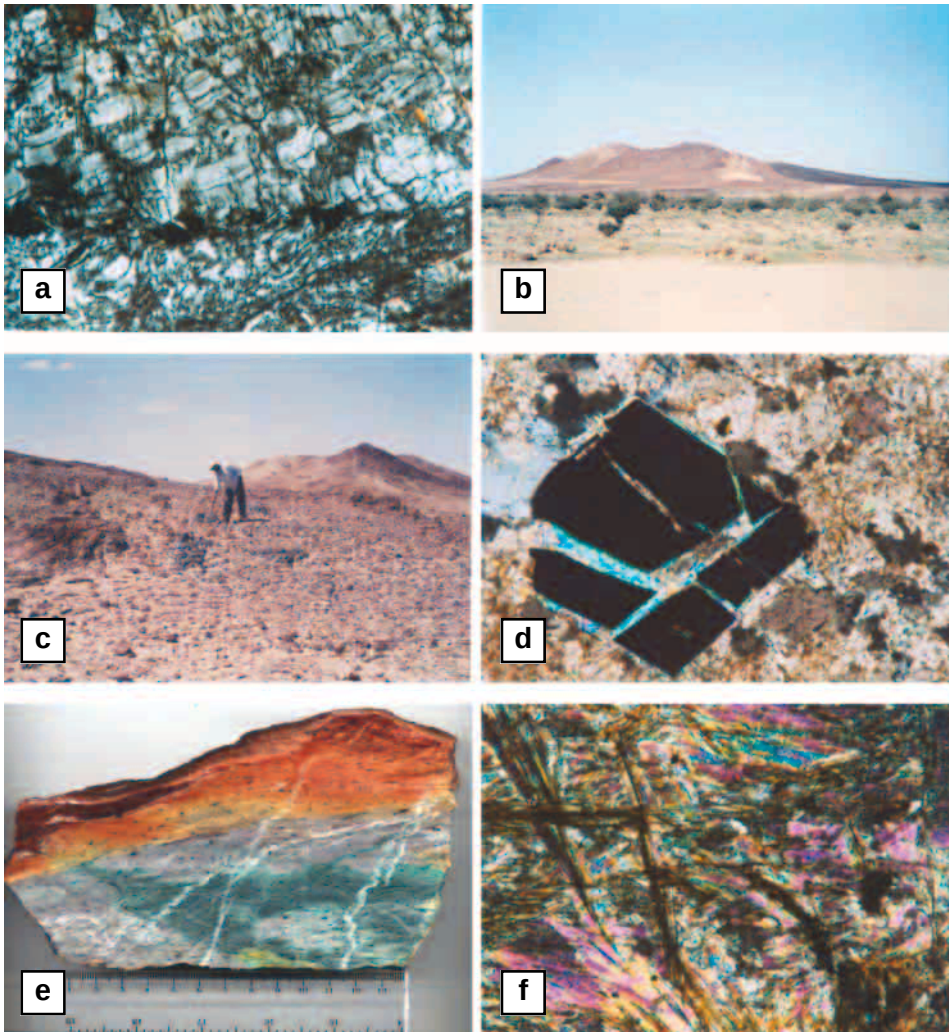

a) Serpentine minerals (antigorite) in sheared serpentine. T.S (Thin Section)., C.N (Crossed Nicol's)., × 25.

b) Listvenite at Jabal Ghadarah (foreground) and late Hulyfah volcanosedimentary rocks (background). Looking south.

c) Mafic fragments incorporated within listvenite at Jabal Ghadarah. Looking north.

d) Development of fuchsite along fractures and boundaries of fractured euhedral chromite crystal in calcite listvenite. T.S., C.N., × 200.

e) Polished slab of fresh listvenite showing fuchsite (green) and opaque minerals (chromite). The upper part of the sample shows oxidation of listvenite.

f) Talc (T) and tremolite (Tr) in metamorphosed serpentine. T.S., C.N., × 100.

Plate 1

ly by chromite, and sulphides (pyrite and pyrrhotite) and magnetite. Chromite occurs as euhedral to subhedral isolated crystals. Magnetite occurs as recrystallized fine euhedral to subhedral grains and usually altered to martite. Sulphides (pyrite and pyrrhotite) occur as fine and disseminated grains. They also form drop-like inclusions within carbonates.

Metagabbros

The metagabbros are mostly observed as isolated large blocks or slices. Small size blocks and fragments (0.5 to 10 m across) are also common. In most cases the metagabbros are intimately associated with serpentinites as large fragments (Plate 2d). The metagabbros are medium to coarse grained, black to dark green in color and composed mainly of plagioclase and amphiboles.

Microscopically, the metagabbros are composed of plagioclase, amphiboles, pyroxene and accessory opaques. Chlorite, calcite, and epidote represent the alteration minerals. Amphiboles, mainly represented by hornblende, occur as large anhedral to subhedral crystals of brownish green color and show corroded and irregular boundaries. These crystals are between 1.5 to 4 mm in length and are randomly oriented (Plate 2e). Some amphibole crystals show well developed twinning (Plate 2e). Actinolite is common and occurs as aggregates of fine fibrous and acicular crystals. The feldspars, mainly represented by plagioclase, occur as coarse to fine anhedral crystals (Plate 2e). Plagioclase is partly or completely enclosed within hornblende forming subophitic and ophitic texture (Plate 2e). These crystals are moderately altered to sericite and carbonate. Sometime fine acicular actinolites are formed at the expense of some plagioclase crystals. Pyroxene crystals are commonly surrounded by amphibole coronas (actinolite and hornblende) (Plate 2f). Ilmenite and rutile are the opaque minerals that have been found in the metagabbros. They constitute about 2% of the total volume of the rock and occur as disseminated fine anhedral grains (0.1 to 0.2 mm size).

Metabasalts

The metabasalt occurs as a large mass at the north central part of the study area. Small size blocks and fragments are also recorded within the listvenites and serpentenites, especially at Jabal Ghadarah. The metabasalt is fine-grained black to green in color and locally show exfoliation (Plate 3a).

Microscopically, these rocks are essentially composed of plagioclase, actinolite and augite. Actinolite, the main constituent mineral of the rock, occurs as fine fibrous and acicular aggregates that seems to have been formed at the expense of pyroxene. The latter forms porphyritic crystals showing lammellar twinning (Plate 3b). Sometime few relicts of pyroxene crystals are observed.

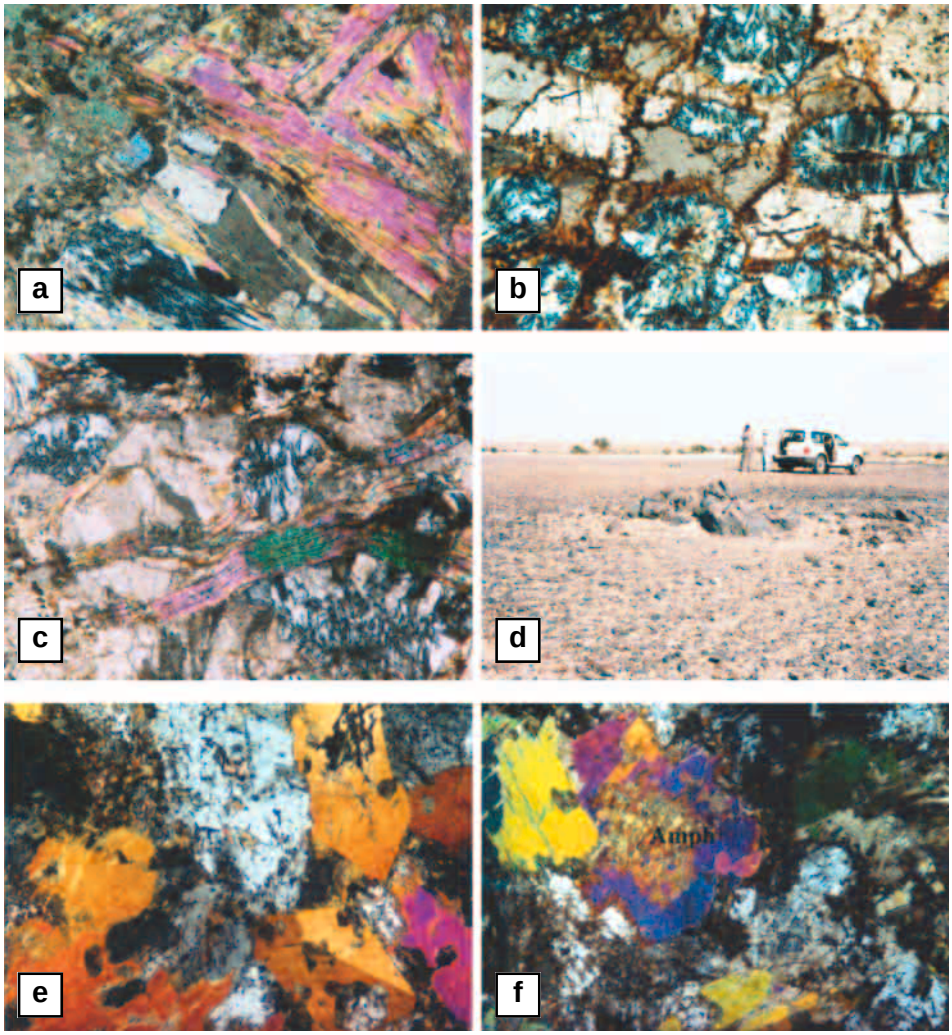

a) Talc in upper right corner and serpentine in left corner incorporated within carbonate groundmass in metamorphosed serpentine. T.S., C.N., × 200.

b) Lizardite pseudomorph after olivine interstitial to magnesite. Notice magnesite is altered to iron oxides along grain boundaries Talc-lizardite listvenite. T.S., C.N., × 200.

c) Talc formed at the expense of magnesite and serpentine minerals in talc-lizardite listvenite. T.S., C.N., × 200.

d) Metagabbro block incorporated within serpentinite host rock.

e) Euhedral twinned hornblende crystals and altered plagioclase. Notice ophitic and subophitic intergrowth of plagioclase and hornblende. Metagabbro. T.S., C.N., × 25.

f) Fine aggregates of amphiboles (Amph) pseudomorph after pyroxene enclosed within a prismatic hornblende. Metagabbro. T.S., C.N., × 25.

Plate 2

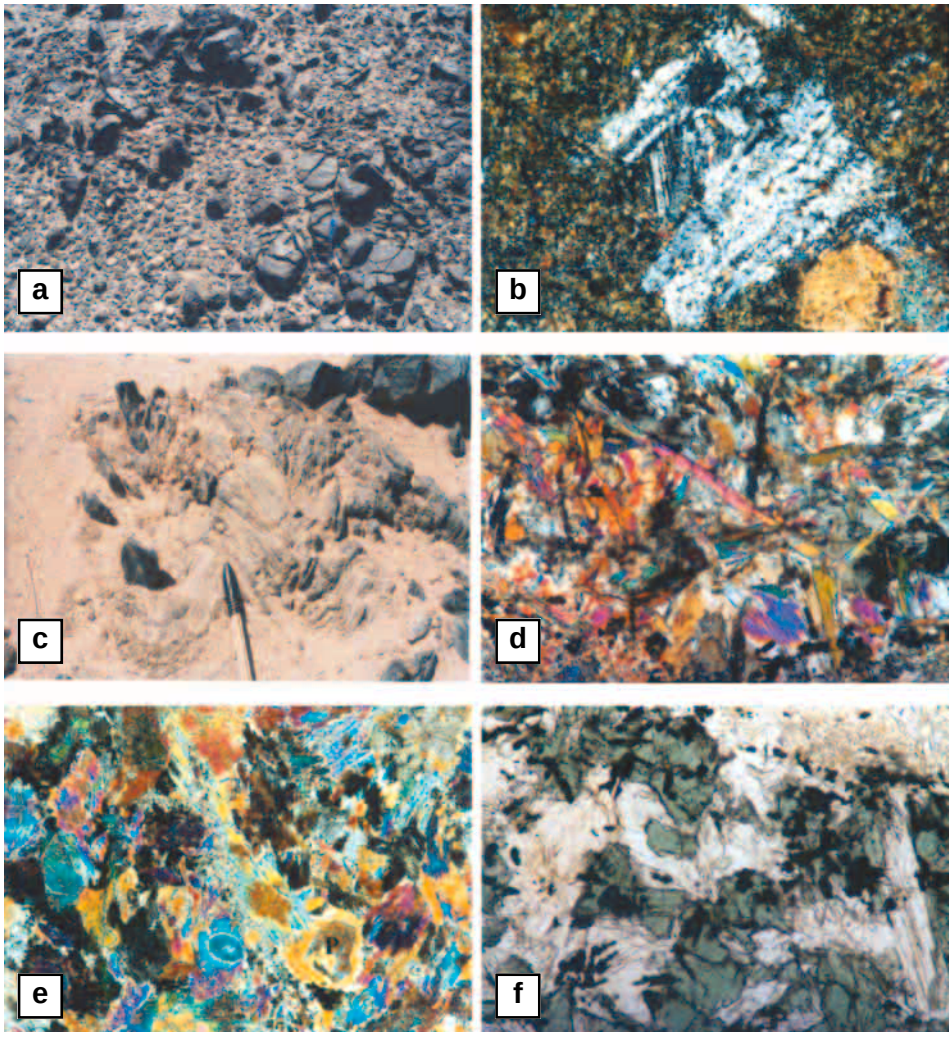

a) Small blocks of metabasalt showing onion-like weathering.

b) Metabasalt showing porphyritic plagioclase crystals embedded in actinolite and epidote groundmass. Notice euhedral augite crystal in the lower right side. T.S., C.N., × 63.

c) Microfolding in highly deformed amphibolite.

d) Spinel bearing amphibolite showing randomly oriented actinolite crystals. T.S., C.N., × 63.

e) Pyroxene relict (P) in the core of actinolite crystals. Spinel-bearing amphibolite. T.S., C.N., × 25.

f) Green spinel associated with magnetite in spinel-bearing amphibolite. T.S., C.N., × 100.

Plate 3

Amphibolites

The amphibolites cropout at the north central and northeastern part of the study area. They form large blocks as well as smaller unmappable elongated fragments. Locally marble lenses occur within the amphibolites. The amphibolites are usually dark green to black and highly foliated, but sometimes massive small blocks are observed. The amphibolites exhibit well developed minor folds related to different phases of deformations (Plate 3c). According to the field relation between the serpentinites and the amphibolites, the latter are interpreted as fragments from the metamorphic sole usually associated with the ophiolitic mélange.

Microscopically two types of amphibolites have been identified: 1) Spinel-bearing amphibolite, and 2) Spinel-free amphibolite.

The spinel-bearing amphibolite, which is believed to be derived from ultramafic rocks (pyroxenite), is mainly made up of actinolite, relict pyroxene and spinel together with accessory opaque minerals (Plate 3d and e). Spinel occurs as coarse anhedral to subhedral aggregated grains and show a distinct green color, isotropic and high relief. Sometime, clusters of spinel aggregates are commonly associated with opaque minerals (magnetite) (Plate 3f and Plate 4a).

Takla and Noweir (1980) recorded the presence of green pleonastic spinel in pyroxenite from ophiolitic ultramafic mass of Jabal El-Rubshi. Also, spinel-bearing amphibolites have been recorded from the area around Zalim (Leistel *et al.*, 1999).

The spinel-free amphibolite, which is believed to be derived from mafic rocks (gabbros), is generally fine grained, greenish to black in color and massive. Under the microscope, these rocks are made up of amphiboles (actinolitic hornblende), plagioclase and accessory opaque minerals. Actinolite is the main constituent of the rock and occurs as fibrous and bladed crystals. Sometimes, actinolitic hornblende forms subidiomorphic to rhombic crystals (Plate 4b). Plagioclase is common and occurs as coarse corroded prismatic crystals partly replaced by acicular actinolite crystals (Plate 4c). Albite twining is still preserved in some plagioclase crystals (Plate 4c).

Marbles

Marbles are recorded at the north central and northeastern part of the study area. They occur as lenses or blocks ranging in size from 0.5-15 m in length and few meters across embedded in serpentinite matrix. The marble lenses are massive to highly fractured and form isolated blocks. They are white to grayish in color and contain black and reddish staining on the weathered surfaces. Mostly, the marble lenses occur as large rock fragments within the serpentinite country

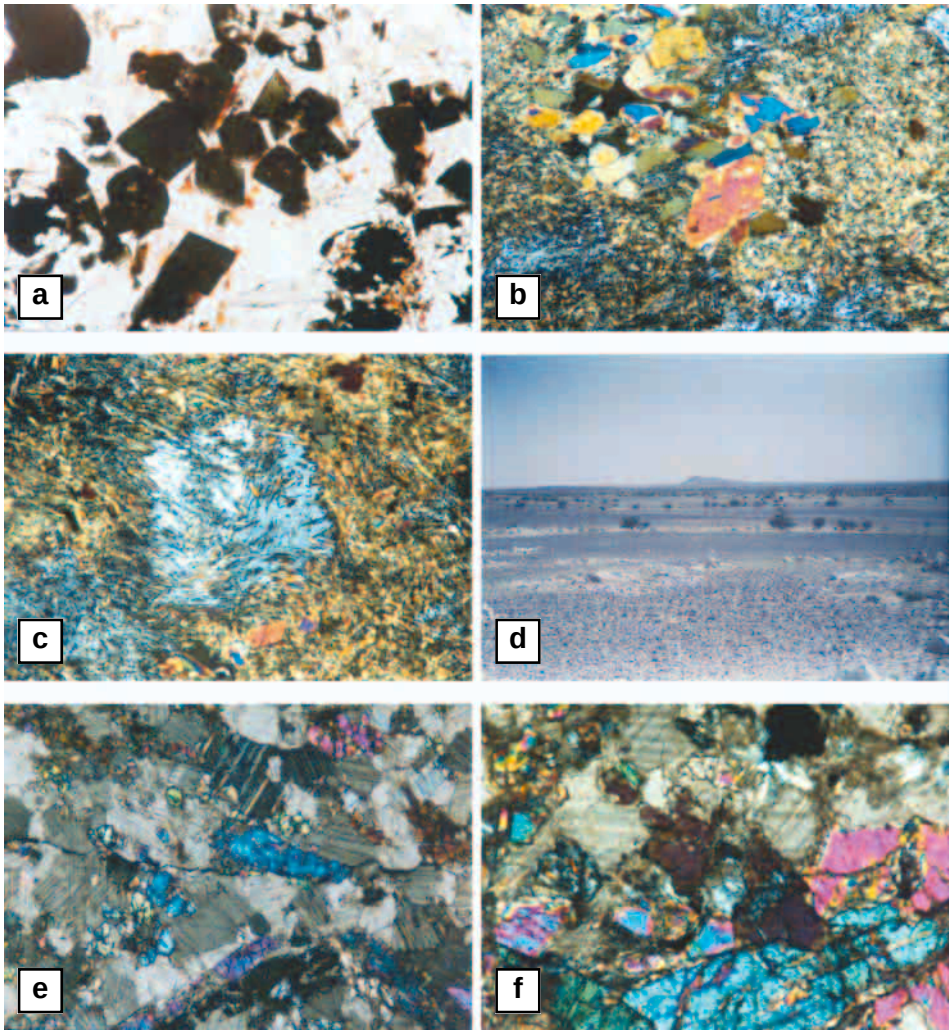

a) Aggregates of euhedral spinel in spinel-bearing amphibolite. T.S., P.P.L., × 200.
b) Amphibolite showing euhedral to subhedral actinolite hornblende crystals (central part of the photo) in a fine actinolite groundmass. T.S., C.N., × 100.
c) Subhedral plagioclase crystals replaced by actinolite. T.S., C.N., × 200.
d) White marble lenses incorporated within serpentinite host rock.
e) Elongated fractured crystals of diopside and rounded to sub-rounded grains of olivine in coarse mosaic aggregates of calcite. Marble. T.S., C.N., × 25.
f) Serpentinized olivine and prismatic diopside crystals in mosaic aggregates of calcite. Marble. T.S., C.N., × 63.

Plate 4

(host) rock (Plate 4d). Microscopically, these rocks consist mainly of calcite with subordinate olivine and diopside. Olivine and diopside appear in marbles, which are thermally affected by the granitic intrusions in the area. Calcite and dolomite are the main constituents of these rocks, and account for more than 70% of the volume of the rock. They occur as mosaic aggregates or clusters of coarse xenomorphic grains (up to 1mm across). They are colorless with rhombohedral cleavage and characteristic low birefringence (Plate 4e). Olivine occurs as fine rounded to subrounded grains ranging in size from 0.1 to 1.7 mm enclosed and interstitial to calcite. Locally olivine is altered to serpentine minerals. Diopside occurs as large, randomly oriented prismatic crystals. They range from 1 to 2.5 mm in length and are commonly cracked (Plate 4f).

Geochemistry of Ophiolitic Mélange Rock Fragments

This section deals with the geochemistry of the metagabbroic, metabasaltic, and amphibolite fragments encountered in the ophiolitic mélange in order to identify their petrochemical character, magma type, and tectonic setting. To achieve this goal, representative samples from the different rock types were analyzed for major oxides and trace elements.

Geochemistry of Metagabbros

The metagabbroic rocks, encountered within the ophiolitic mélange in the studied area have been sampled and analyzed for major oxides and trace elements, and were subjected for detailed petrographic investigation. The results of the major oxides and trace elements analyses of fourteen metagabbroic rock samples are listed in Table 1.

Table 1. Chemical analyses of metagabbros.

Sample	JGN 3A	JGN 3B	JGN 4B	JGN 4D	JGN 26	JGN 30
SiO_2	47.40	49.70	43.35	45.25	51.60	47.35
TiO_2	0.15	0.26	0.03	0.27	1.65	1.26
Al_2O_3	15.62	13.55	16.52	16.60	15.85	14.30
Fe_2O_3	6.98	9.73	3.81	12.97	8.80	7.76
MnO	0.23	0.29	0.16	0.22	0.15	0.13
MgO	13.60	10.60	10.10	7.92	3.56	5.06
CaO	12.80	11.65	20.50	12.50	6.20	6.90
Na_2O	0.82	2.01	0.96	1.58	2.90	2.82
K_2O	0.29	0.49	0.30	0.56	1.36	5.15
P_2O_5	0.02	0.06	0.02	0.04	0.26	0.44
SO_3	0.05	0.05	0.06	0.05	0.06	0.03
L.O.I	1.64	1.43	4.26	2.20	7.01	9.00
SUM	99.60	99.82	100.07	100.16	99.40	100.20

Table 1. Contd.

Sample	JGN 3A	JGN 3B	JGN 4B	JGN 4D	JGN 26	JGN 30
			ppm			
Cr (10)*	647	955	590	136	9	233
Ni (10)	222	299	162	149	42	101
Co (5)	32	54	30	48	32	29
V (10)	73	176	66	527	196	185
Cu (5)	33	25	7	43	15	38
Pb (10)	6	5	1	–	1	10
Zn (5)	51	79	28	63	91	83
Bi (10)	–	–	–	1	1	1
Cd (5)	4	4	2	5	3	3
Sn (50)	11	11	8	12	4	4
W (10)	–	–	–	–	6	13
Mo (5)	6	7	4	5	4	6
As (50)	21	39	9	47	108	234
Sb (10)	–	2	–	4	5	4
Ag (1.0)	–	–	–	–	–	0.7
Au (0.01)	–	–	0.01	0.01	–	0.02
Ba (10)	73	93	56	98	48	322
Sr (5)	200	42	233	207	142	156
Li (10)	11	–	23	21	–	39
Nb (20)	5	8	3	5	1	10
Zr (250)	10	59	6	20	5	94
Y (20)	3	12	2	3	1	18
La (20)	–	4	–	–	–	9
Ce (10)	2	2	–	1	6	20
B (10)	21	31	27	33	18	29
Be (2)	–	–	–	–	–	–

*Detection limit. (–) Below detection limit.

Table 1. Contd.

Sample	JGN 74	JGN 101B	JGN 102	JGN 103	JGN 105	JGN 107
SiO_2	52.90	48.2	48.5	29.7	48.2	56.5
TiO_2	0.08	1.55	0.57	0.53	0.57	0.09
Al_2O_3	5.15	15.3	6.9	18.5	7.3	5.5
Fe_2O_3	9.43	12.3	9.6	12.4	9.2	11.3
MnO	0.22	0.21	0.16	0.28	0.16	0.18
MgO	21.20	5.5	20.4	24.3	19.6	18.8
CaO	7.28	12.8	8.2	1.6	8.5	4.8
Na_2O	0.20	2.23	0.62	0.14	0.51	0.51
K_2O	0.08	0.3	0	0	0	0.1
P_2O_2	0.03	0.2216	0.1069	0.3378	0.1033	0.0385

Table 1. Contd.

Sample	JGN 74	JGN 101B	JGN 102	JGN 103	JGN 105	JGN 107
SO_3	0.06	0.04	0.05	0.06	0.03	0.06
L.O.I	3.64	0.83	4.43	11.86	4.82	1.55
SUM	100.27	99.4816	99.5369	99.7078	98.9933	99.4285
			ppm			
Cr	2751	806	2002	210	2202	3033
Ni	648	309	869	235	1206	636
Co	71	61	68	44	73	69
V	103	355	139	343	149	118
Cu	9	91	13	61	37	9
Pb	–	–	–	–	–	–
Zn	77	89	64	106	70	85
Bi	–	4	–	–	–	–
Cd	2	5	5	4	5	5
Sn	11	7	16	14	19	21
W	–	–	–	–	–	–
Mo	6	6	5	6	5	5
As	168	21	52	57	25	53
Sb	2	2	2	–	–	–
Ag	–	–	–	–	–	–
Au	–	–	–	–	–	–
Ba	421	223	39	295	24	62
Sr	727	162	44	99	59	45
Li	15	4	–	–	–	7
Nb	5	17	14	8	15	6
Zr	101	99	61	47	64	31
Y	20	27	11	9	12	2
La	14	6	4	3	5	–
Ce	30	13	9	8	11	1
B	18	6	15	14	14	11
Be	–	–	–	–	–	–

It is well known that, recognition of magma type, its chemical nature and its behavior on differentiation, aptly help to decipher the tectonic setting of the rocks. The magma type of the concerned metagabbroic rocks is clarified through the following relationships (Fig. 3a, b and c):

a. SiO_2 vs. (Na_2O+K_2O) diagram (Fig. 3a) of Mac Donalds and Katsura (1964) shows that the metagabbros fall within the field of tholeiitic suite.

b. SiO_2 vs. (Na_2O+K_2O) diagram (Fig. 3b) of Irvine and Baragar (1971), reveals that the metagabbroic samples are plotted within the field of subalkaline magma.

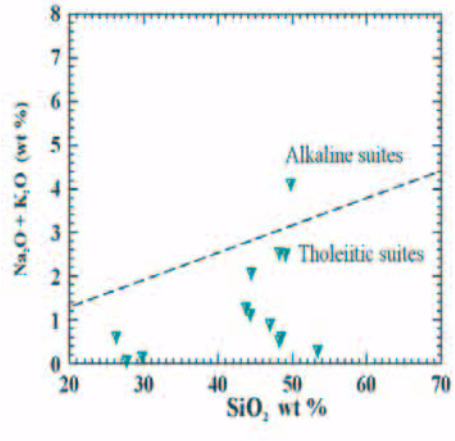

Fig. 3(a). Na_2O+K_2O *vs.* SiO_2 diagram for metagabbroic rocks (Mac Donalds and Katsura, 1964).

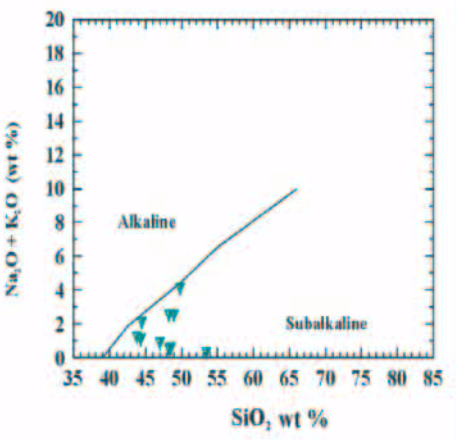

Fig. 3(b). Na_2O+K_2O *vs.* SiO_2 diagram for metagabbroic rocks (Irvine and Baragar, 1964).

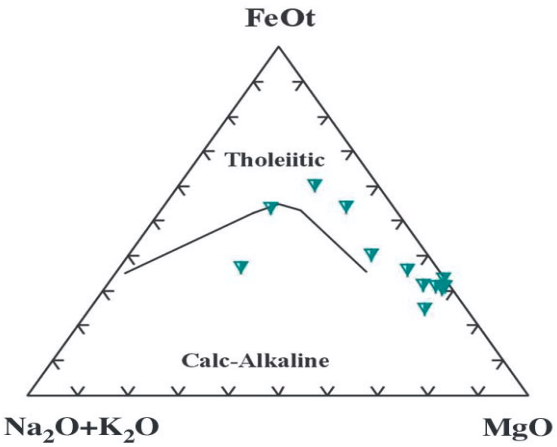

Fig. 3(c). AFM ternary diagram for the metegabbroic rocks (Irvine and Baragar, 1971).

c. On the AFM diagram (Fig. 3c) of Irvine and Baragar (*op. cit*.), the metagabbroic samples show a tholeiitic trend.

The ocean floor affinity of the metagabbros is not fully revealed by the Ti/100-Zr-Sr/2 (Pearce and Cann, 1973) (Fig. 4). The scatter of the data can be explained in term of metamorphism and alteration. Also, the scatter can be attributed to the coarse grained nature of the rocks (cumulates) and the chemistry of metagabbros does not represent the original composition of the magma.

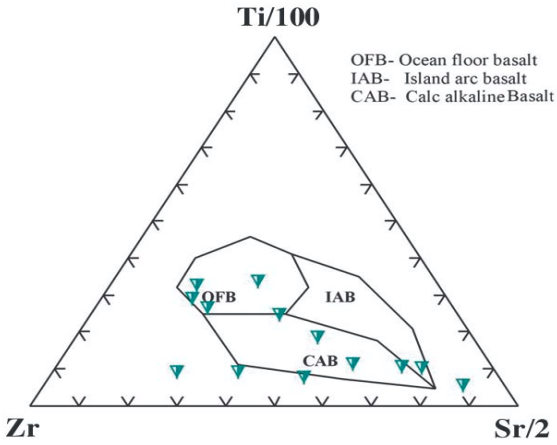

Fig. 4. Ti/100-Zr-Sr/2 ternary diagram for the metagabbroic rocks (Pearce and Cann, 1973).

Geochemistry of Metabasalts

The metabasaltic rocks present in the study area are considered as a component of the ophiolitic mélange rocks. Eight samples, were analysed for major oxides and trace elements and the results are given in Table 2.

The metabasaltic rocks are chemically classified using the SiO_2 vs. Na_2O+K_2O (total alkalies) and K_2O vs. SiO_2 diagrams. The plotting of the data coincides completely with the microscopic identification.

Total alkalies vs. SiO_2 diagram (Le Maitre *et al.*, 1989) is used to differentiate between the different types of volcanic rocks. Most of the metabasalt samples are plotted in the basalt field (Fig. 5).

Irvine and Baragar (1971) used the relationship between SiO_2 and total alkalies for the distinction between the alkalic and subalkalic magma (Fig. 6). The majority of the metabasalt samples are plotted in the subalkaline field, while two samples are within alkaline field close to the subalkaline field.

Irvine and Baragar (*op. cit*.) used the AFM ternary diagram in order to discriminate between calc alkaline magma (CA) and the tholeiitic magma (TH) (Fig. 7). The majority of the metabasalt samples show Fe enrichment indicative of a tholeiitic trend.

On SiO_2 vs. FeOt/MgO diagram (Miyashiro, 1974) the majority of the analyzed metabasalt samples are plotted in the tholeiite field (Fig. 8).

Pearce (1975) used the Cr against Ti diagram (Fig. 9), to differentiate between the Ocean floor basalt (OFB) and the low potassium tholeiite (LKT). The

Table 2. Chemical analyses of metabasalts.

Sample	JGN 37	JGN 47	JGN 50A	JGN 58	JGN 64	JGN 76	JGN 114	JGN 116
SiO_2	47.86	49.00	50.25	52.50	49.00	44.75	52.60	49.80
TiO_2	1.22	1.15	1.80	1.10	1.00	1.60	2.30	0.60
Al_2O_3	14.40	13.62	12.70	17.44	14.23	14.97	14.90	16.20
Fe_2O_3	8.60	9.98	11.15	9.65	10.87	12.22	9.50	11.30
MnO	0.14	0.18	0.21	0.17	0.27	0.22	0.10	0.30
MgO	5.98	4.60	5.65	4.90	7.40	7.60	3.40	5.70
CaO	7.30	10.48	7.84	6.44	12.34	14.10	6.30	11.80
Na_2O	2.97	1.16	3.32	3.89	2.86	1.31	3.59	3.24
K_2O	1.05	1.15	0.47	0.12	0.31	0.69	2.50	0.40
P_2O_5	0.35	0.13	0.16	0.30	0.09	0.15	0.97	0.06
SO_3	0.08	0.08	0.06	0.09	0.08	0.06	0.06	0.05
L.O.I	9.38	8.67	6.71	3.50	1.43	1.48	4.45	0.66
SUM	99.33	100.20	100.32	100.10	99.88	99.15	100.61	100.06
				ppm				
Cr	387	193	40	50	306	317	212	632
Ni	130	77	65	56	99	119	56	97
Co	32	41	41	37	47	50	31	42
V	197	281	340	279	320	360	192	248
Cu	28	78	92	47	126	139	42	118
Pb	12	4	5	14	–	–	5	–
Zn	77	75	86	92	75	100	129	60
Bi	3	4	4	5	2	5	2	6
Cd	3	3	5	4	1	1	4	5
Sn	13	14	13	13	–	–	20	22
W	–	10	6	8	–	–	–	–
Mo	6	6	8	7	–	–	4	7
As	85	86	75	68	41	81	21	32
Sb	9	18	10	24	–	–	–	–
Ag	–	0.7	0.2	0.9	–	–	–	–
Au	–	–	–	–	–	–	–	–
Ba	981	275	296	209	139	312	1776	323
Sr	609	159	212	1018	225	290	1164	163
Li	42	32	16	21	4	11	37	11
Nb	9	3	6	9	9	4	19	11
Zr	158	65	203	108	54	88	76	30
Y	18	20	25	20	18	22	17	15
La	15	2	4	15	–	4	37	–
Ce	34	3	9	34	5	9	79	1
B	22	29	21	24	17	19	4	13
Be	–	–	–	–	–	–	–	–

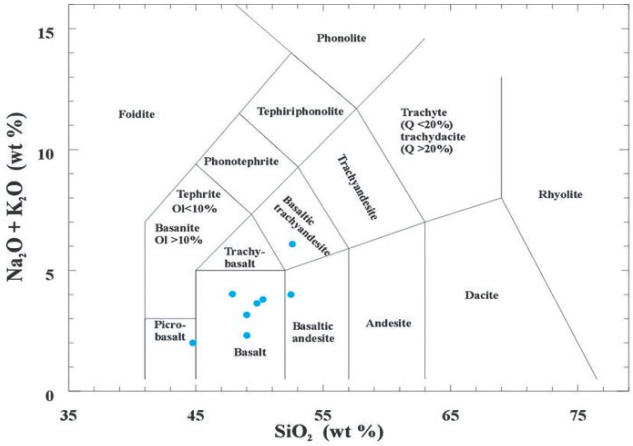

Fig. 5. Na_2O+K_2O *vs.* SiO_2 diagram for the metabasaltic rocks (Le Maitre *et al.*, 1989).

studied metabasalt samples are plotted within the OFB except one sample, which is plotted in LKT field close to the OFB filed.

Shervais (1982) used the V vs. Ti/1000 binary diagram to distinguish between the Ocean floor (OFB) and the Island arc (ARC) basalt. Accordingly, most of metabasalt samples are plotted within the OFB field, while two samples are plotted within the Island arc field close to the OFB field (Fig. 10).

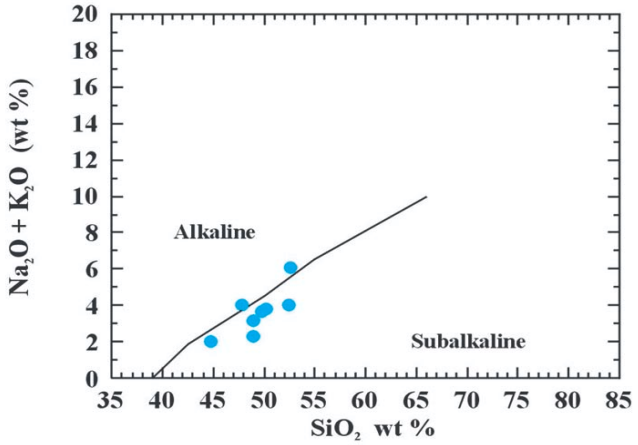

Fig. 6. Na_2O+K_2O *vs.* SiO_2 diagram for the metabasaltic rocks (Irvin and Baragar, 1971).

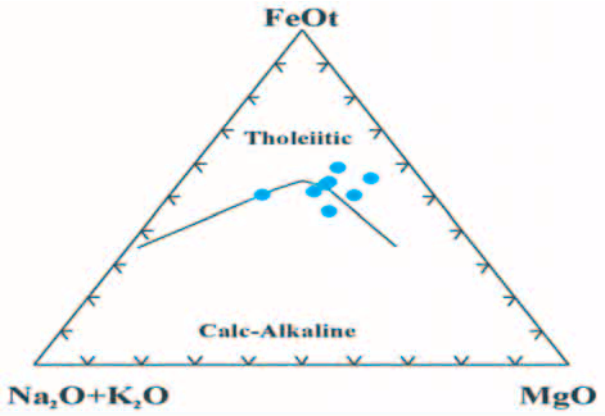

Fig. 7. AFM ternary diagram for the metabasaltic rocks (Irvine and Baragar, 1971).

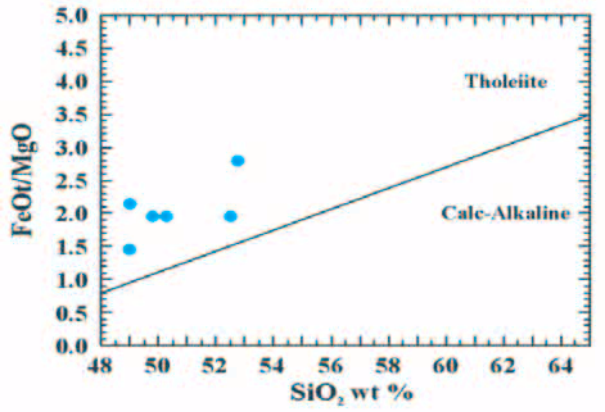

Fig. 8. FeOt/MgO *vs.* SiO_2 diagram for metabasaltic rocks (Miyashiro, 1974).

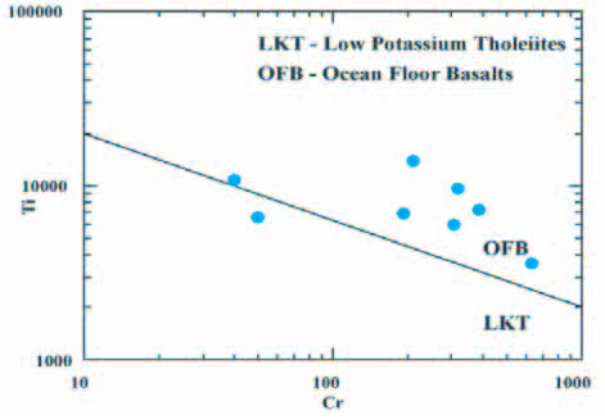

Fig. 9. Ti *vs.* Cr diagram for the metabasaltic rocks (Pearce, 1975).

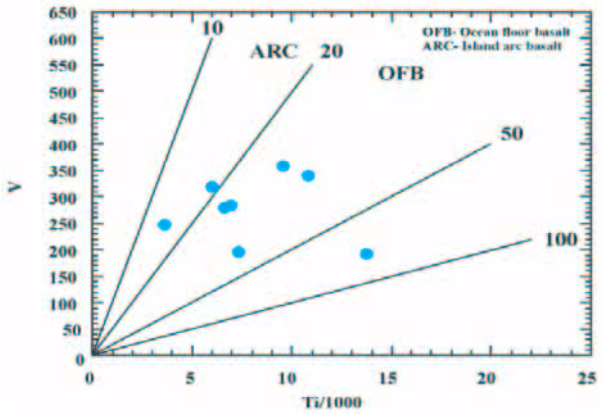

Fig. 10. V *vs.* Ti/1000 diagram for the metabasaltic rocks (Shervais, 1982).

Geochemistry of the Amphibolites

The amphibolites, which are encountered in the ophiolitic mélange in the study area have been sampled for detailed petrography and geochemical studies to clarify their nature and parent rocks. Eight representative rock samples were analysed for the major and trace elements. The results are tabulated in Table 3.

Table 3. Chemical analyses of amphibolites.

Sample	JGN 46	JGN 78	JGN 79	JGN 80	JGN 81	JGN 121	JGN 122C	120A
SiO_2	48.80	51.30	49.60	43.70	47.00	51.60	27.60	36.50
TiO_2	1.34	1.26	1.08	1.55	1.63	1.33	3.07	0.88
Al2O3	12.62	13.51	8.95	13.25	16.00	11.80	19.30	15.70
Fe2O3	15.15	10.22	10.42	12.95	12.70	12.30	17.50	13.00
MnO	0.31	0.22	0.18	0.22	0.20	0.18	0.30	0.14
MgO	7.46	7.45	18.90	19.40	5.35	12.90	20.50	24.20
CaO	7.14	8.92	7.40	4.48	14.40	6.20	1.10	1.60
Na2O	2.89	5.37	0.32	0.32	1.32	1.82	0.09	0.16
K2O	1.18	0.27	0.07	0.09	0.35	0.10	0.00	0.00
P2O5	0.14	0.12	0.20	0.17	0.22	0.20	0.34	0.18
SO3	0.06	0.07	0.08	0.04	0.04	0.05	0.05	0.05
L.O.I	2.82	1.06	2.14	2.88	0.72	1.52	9.82	7.07
SUM	99.91	99.77	99.34	99.05	99.93	100.00	99.67	99.48
				ppm				
Cr	95	420	1387	535	848	1065	370	121
Ni	79	203	996	237	322	823	311	150
Co	52	51	59	44	64	61	65	45
V	426	366	194	308	395	260	471	92
Cu	95	53	62	10	96	155	16	9
Pb	8	–	–	–	–	–	–	–

Table 3. Contd.

Sample	JGN 46	JGN 78	JGN 79	JGN 80	JGN 81	JGN 121	JGN 122C	120A
Zn	109	84	57	56	94	89	117	82
Bi	2	8	–	2	7	1	–	–
Cd	4	1	2	1	1	6	7	5
Sn	20	–	3	–	–	27	25	18
W	13	–	–	–	–	–	–	–
Mo	8	2	5	4	2	6	5	5
As	92	67	109	102	69	57	52	21
Sb	11	7	–	17	4	–	–	–
Ag	0.8	–	–	–	0.5	–	–	–
Au	–	–	–	–	–	–	–	–
Ba	355	178	109	80	164	170	152	24
Sr	423	213	55	65	196	184	106	36
Li	11	4	6	20	8	3	4	8
Nb	5	5	11	2	12	16	17	14
Zr	81	65	97	102	92	95	204	265
Y	33	25	19	25	28	24	58	34
La	1	–	9	6	6	6	9	26
Ce	1	6	20	13	13	13	19	55
B	15	12	14	18	15	11	12	16
Be	–	–	–	–	–	–	–	–

The studied amphibolites are remarkably of mafic characters as evident from their low contents of SiO_2 and alkalies, and high contents of Fe_2O_3, MgO, CaO and TiO_2. These chemical characteristics also point out the mafic nature of their parent rocks. The petrographic study reveals the presence of two types; 1) Spinel-amphibolite and 2) Spinel-free amphibolite. The relatively high content of the TiO_2 (ranging between 1 and 3.07%) collaborates the ore microscopic study, which indicates the dominance of ilmenite. The results of chemical analyses were plotted on SiO_2-CaO-MgO and Al_2O_3-CaO-MgO ternary diagrams (Fig.11a and b). From these diagrams, two groups can be distinguished. The 1st group is characterized by higher MgO and low CaO and SiO_2. The 2nd group shows higher SiO_2 and CaO and lower MgO. Such grouping is confirmed petrographically where the 1st group was found to be spinel-bearing and believed to be formed after ultramafic (pyroxenites) protolith, while the 2nd group was formed after a mafic (metagabbros) protolith.

Furthermore, the Zr/Ti versus Ni and P_2O_5/TiO_2 versus MgO/CaO relationships, which were used by many authors (*e.g.*, Miller and Barr, 2000) to distinguish between ortho (igneous) and para (sedimentary) amphibolites indicate that the studied amphibolites are of igneous protolith (Fig.12a and b).

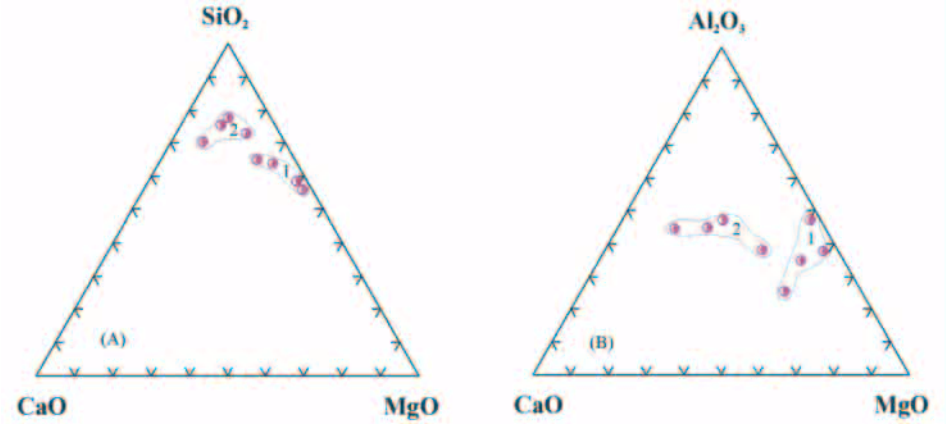

Fig. 11. SiO_2-CaO-MgO (A) and Al_2O_3-CaO-MgO (B) ternary diagrams for spinel-bearing (1) and spinel free (2) amphibolites.

The Zr versus TiO_2 diagram was used by Hallberg (1985) to distinguish between the different types of plutonic rocks. The majority of amphibolite samples were plotted within the field of mafic-ultramafic rocks, (Fig. 13).

The magma type of the amphibolite protolith can be clarified from the relation between the total alkalies and SiO_2 (Irvine and Baragar, 1971) for the distiniction between the alkaline and subalkaline magmas. Most of the amphibolite samples are plotted within or close to the field of subalkaline magma (Fig. 14).

Irvine and Baragar (*op. cit*.) used the AFM ternary diagram in order to discriminate between the calc-alkaline magma (CA) and the tholeiitic (TH) one. The majority of the amphibolite samples show tholeiitic trend (Fig. 15).

The tectonic setting of the protolith of the amphibolites is defined through the V versus Ti/1000 binary diagram, which distinguishs between the ocean floor basalt (OFB) and the island arc (ARC) basalt (Shervais, 1982). Accordingly, most of the amphibolite samples plot within the OFB field (Fig. 16).

Pearce and Cann (1973) used the Ti/100-Zr-Y*3 ternary diagram to identify the different tectonic setting of basaltic magma. The majority (6 samples) of studied amphibolite samples plot within the field of the ocean floor (Fig.17).

In conclusion, based on the mineralogical composition as well as geochemical characters, the studied amphibolites were derived by metamorphism of mafic (metagabbro)-ultramafic (pyroxenite) protolith and can be considered as the metamorphic sole or subophiolitic amphibolites similar to those described from Oman (Lippard *et al*., 1986), Egypt (Abd El-Naby *et al*., 2000) and Newfoundland (Williams and Smythe, 1973).

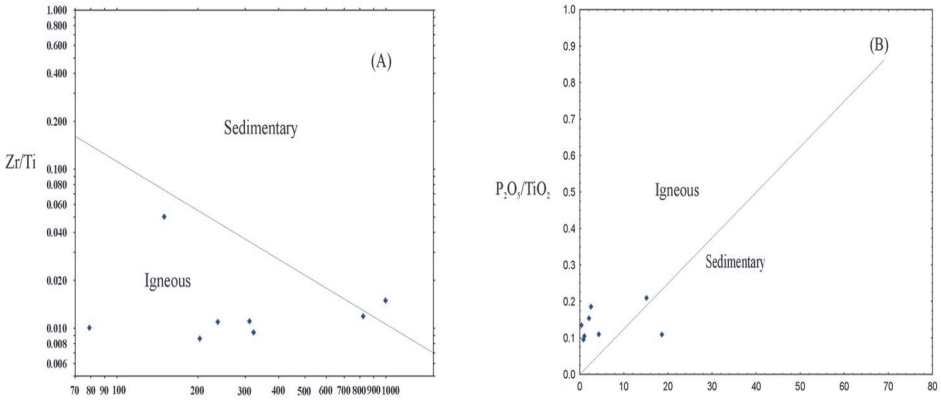

Fig. 12. Zr/Ti *vs.* Ni (A) and P_2O_5 *vs.* MgO/CaO (B) for amphibolites. Dividing lines in A and B (after Wernner, 1987).

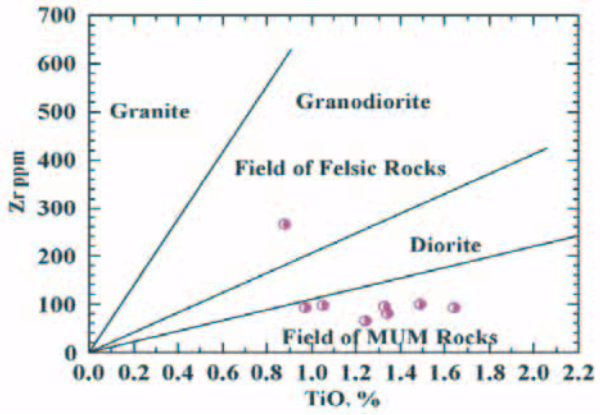

Fig. 13. Zr *vs.* TiO_2 diagram for amphibolites (Hallberg, 1985).

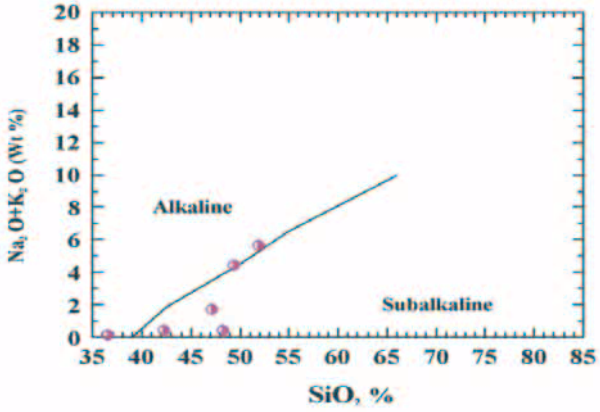

Fig. 14. Na_2O+K_2O *vs.* SiO_2 diagram for the amphibolites (Irvine and Baragar, 1971).

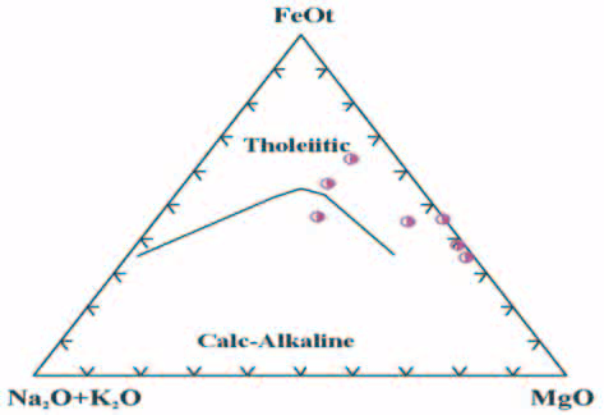

Fig. 15. AFM ternary diagram for the amphibolite rocks (Irvine and Baragar, 1971).

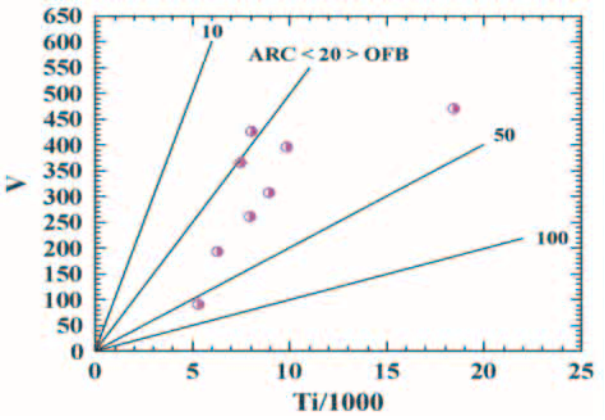

Fig. 16. V *vs.* Vi/1000 diagram for the amphibolites (Shervais, 1982).

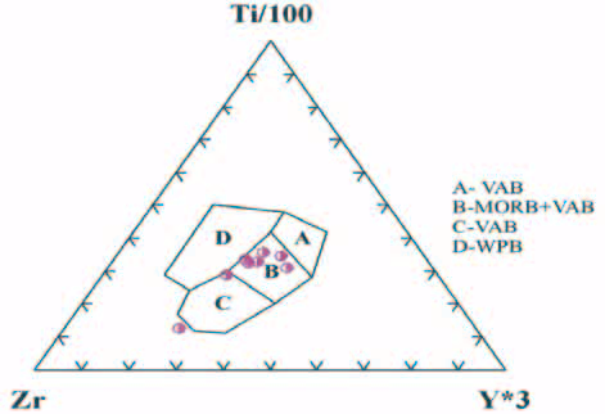

Fig. 17. Ti/100-Zr-Y*3 ternary diagram for the amphibolites (Pearce and Cann, 1973).

Geochemistry of Chromite

The petrographic studies of the metaultramafites and associated rock fragments revealed that the area was subjected to green schist- amphibolite facies metamorphism. Such a metamorphism obliterated the primary minerals of the ultramafic protolith, however, chromite survived metamorphism and can be used as a petrogenetic indicator (Irvine, 1965, 1967 and 1976; Dick, 1977; Evans and Frost, 1975; Fisk and Bence, 1980; Dick and Bullen, 1984 & Ahmed *et al*., 2001).

The studied serpentinites and listvanites contain chromite as disseminations as well as massive lensoid aggregates (chromitites). Chromite crystals are highly fractured, brecciated and altered along the crystal boundaries and fractures into magnetite with fresh remnants at the core displaying the characteristic brown color.

Representative crystals were analyzed for major oxides by SEM-EDX and the results are listed in Table 4. Chromite shows a wide compositional range where Cr_2O_3% ranges from 51.18 to 60.58 and Al_2O_3 content from 2.20 to 17.73 % and is comparable to chromite from podiform chromitites (Fig. 18). The Cr# varies from 0.67 to 0.82 (Table 4) and is comparable to those reported by Ahmed *et al.* (2001) from Proterozoic ophiolites from Egypt. The Mg# is generally variable and ranges from 0.12 to 0.94.

Table 4. Chromite major oxides content.

Wt %	1	2	3	4	5
Cr_2O_3	60.58	55.27	53.89	51.18	53.26
Fe_2O_3	22.88	20.38	22.11	31.71	18.52
Al_2O_3	9.12	14.93	15.18	14.90	17.73
MgO	7.42	8.97	9.25	2.20	10.14
Total	100.00	100.00	99.43	99.99	100.01
Cr#	0.82	0.71	0.70	0.70	0.67
Mg#	0.94	0.46	0.47	0.12	0.36

The close similarity of Pan-African (Upper Proterozoic) peridotites to Phanerozoic peridotites from present day fast-spreading ridges suggests that the geothermal gradients, which control the genesis of the crust-mantle rocks, have not significantly changed since the late Proterozoic era (Brown, 1979 and Ahmed *et al.*, 2001).

Dick and Bullen (1984) classified peridotites from ophiolitic complexes, based on chromite chemistry, as type I where the chromite composition is com-

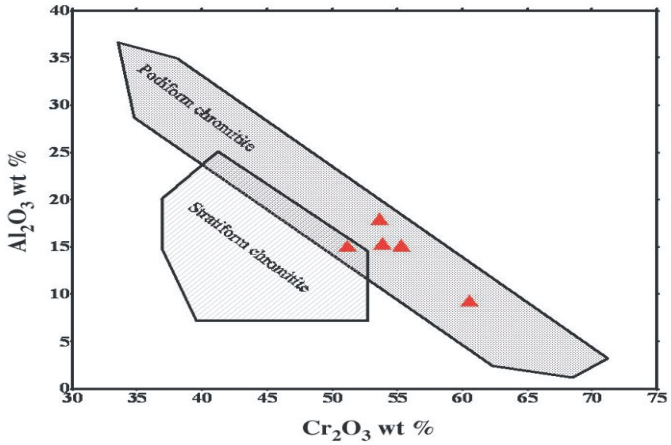

Fig. 18. Variation of Cr_2O_3 *vs.* Al_2O_3 of chromite in Ghadarah peridotites. Compositional fields of podiform and stratiform chromitites after Bonavia *et al.* (1993).

parable to chromite from peridotites dredged from the present day mid-ocean ridge rocks (Cr# > 0.6), type III where the chromite composition (Cr# < 0.6) is different from type I and resembles peridotites from island-arc terranes, and as type III where the chromite compostion overlaps type I and III and is of composite origin (island arc on oceanic crust).

On the Cr# (Cr × 100)/(Cr + Al) *vs.* Mg# (Mg × 100)/ (Mg + Fe^{2+}) diagram (Fig. 19), the chromite from the study area is similar to chromite of the type-III peridotites suggesting the formation of the peridotites in an arc-related setting.

The proterozoic ophiolitic rocks of the Arabian Shield were studied by Al Shanti and El-Mahdy (2001) and five terranes sutured by ophiolitic rocks were recognized, and three types of collision between these terranes were suggested: 1) Island arc – Island arc (*e.g.*, Bir Umq – Jabal Thurwah), 2) Island arc – Continental margin (*e.g.*, Bir Tuluha-Hamdah), and 3) Collision between two continental blocks. In the first two types of collision arc volcanics and ophiolitic rocks are juxtaposed along the sutures, while in the latter the ophiolitic rocks are not associated with arc volcanics. The ophiolitic rocks in the 3rd type were interpreted as a squeezed oceanic crust formed in a rift zone between two continental blocks. Johnson *et al.* (2003) mapped arc related volcanics and intrusive rocks in association with Halaban ophiolitic complex (Fig. 11), thus, it resembles the other sutures. Moreover, chromite from Halaban ophiolitic complex plot close to the fields of chromian spinels from bonatites and forearc ophiolites (Johnson *et al.*, 2003)

The chromites from the Arabian Shield ophiolitic rocks show a high variation in Cr and Al (Cr# for the majority of samples ranges between 0.6 and 0.8)

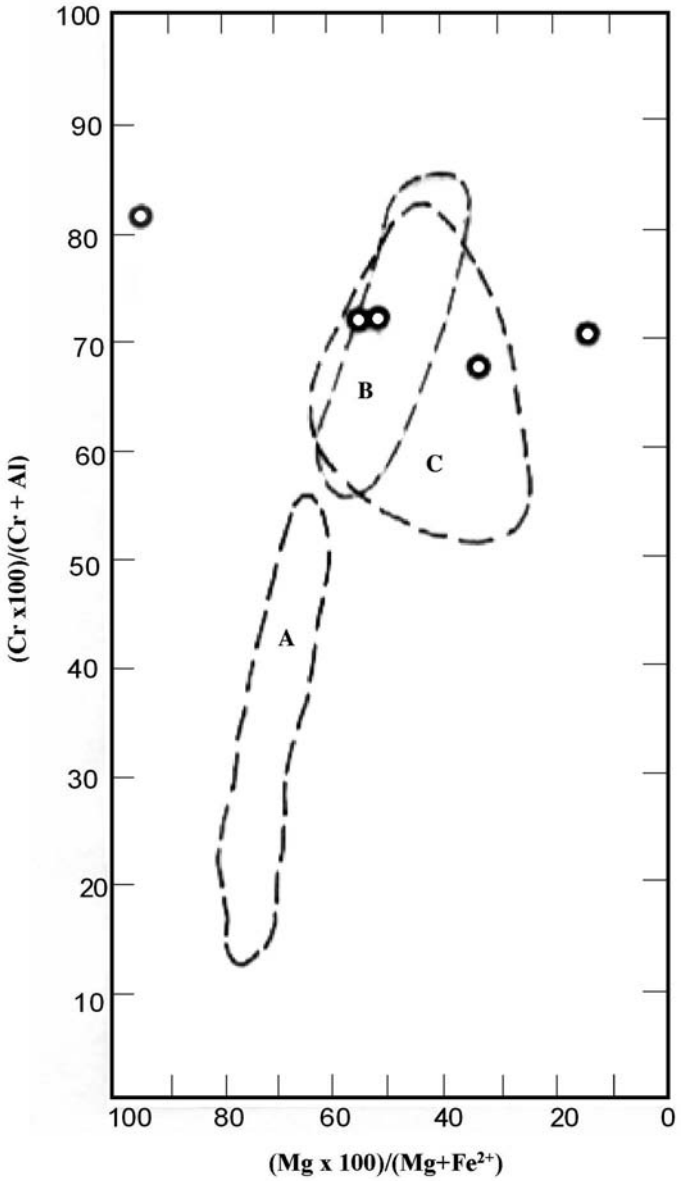

Fig. 19. Composition of the chromite from the study area. Fields A, B and C after Dick and Bullen (1984). Field A for mid-ocean ridge peridotites, fields B and C for type III Alpine peridotites (Field B for peridotites from Twin Sisters, and C for peridotites from Troodos Complex).

and are similar to chromites of the podiform (Alpine) type (El-Mahdy and Al Shanti, 2001). Also, on the basis of chromite chemistry, forearc-setting has been suggested for Jabal Ess and Bir Tuluhah ophiolites (Johnson *et al.*, 2003), and Jabal Thurwah ophiolite complex (Nassief *et al.*, 1984).

Bakor *et al.* (1976) studied the mafic-ultramafic complex from Jabal Al Wask (Saudi Arabia) and was considered as an ophiolite possibly formed in a back arc environment and the ultramafic zones are sutures between island arcs during the cratonization of the Arabian Shield.

Based on chromite chemistry and petrological data, Azer and Khalil (2006) suggested an environment akin to a suprasubduction zone in a back arc basin for serpentinites and associated chromitite lenses from Wadi Sodmein area, Nubian shield, Egypt.

Summary and Conclusions

The study area comprises the following rock units (from the oldest to the youngest): the ophiolitic mélange rocks, the early Hulyfah volcanosedimentary rocks, the late Hulyfah volcanosedimentary rocks, the syn- to late-orogenic intrusive rocks, the Murdamah volcano-sedimentary rocks, the post orogenic intrusive rocks and dikes.

The term ophiolitic mélange is introduced for the first time to describe the geology of the study area. It consists of ultramafic rocks (serpentinites and listvenite), metagabbros, metabasalts, marble lenses and amphibolites. The described ophiolitic mélange occupies the hanging wall of the major Bir Tawilah thrust fault. The footwall is occupied by the late Hulyfah volcanosedimentary rocks. The zone of the listvenite along the Bir Tawilah major thrust fault marks the contact between the late Hulyfah volcanosedimentary rocks and the ophiolitic mélange. The sheared serpentenites host the components of the ophiolitic mélange. Based on their major and trace element compositions, the metagabbro and metabasalt rock fragments, are tholeiitic in character and of ocean floor-affinity. The amphibolites are found to be orthoamphibolites of igneous protolith. The protolith of these amphibolites is tholeiitic in character and of ocean-floor affinity and was derived by metamorphism of mafic (metagabbro)-ultramafic (pyroxenite) protolith.

The chemistry of chromite from Jabal Ghadarah area is similar to podiform chromitites, to chromite from Proterozoic ophiolitc peridotites and can be grouped with chromite from type III peridotites formed in an arc-related setting.

References

Abd El-Naby, H., Frisch, W. and **Hegner, E.** (2000) Evolution of the Pan-African Wadi Haimur metamorphic sole, Eastern Desert, Egypt, *Journal of Metamorphic Geology*, **18:** 6.

Abdel Wahed, M. (1985) *Structural and Petrological Studies on the Migif-Hafafit Gneisses*, Eastern Desert, Egypt. Ph. D. Thesis, Cairo Univ., Egypt.

Abdel Wahed, M., Eldougdoug, A., Awadallah, M.F. and **Hamimi, Z.** (1986) On the relation between the ophiolitic mélange and the banded iron-formation of Gabal Elhadid area, Central Eastern Desert, Egypt. *Ann. Geol. Surv*., **XVI:** 57-67.

Agar, R.A. (1984a) Geology of Zalim quadrangle, *Sheet 22 F Kingdom of Saudi Arabia Deputy Ministry for Mineral Resourses. Open-File-Report DGMR-OF-**04-01***.

Agar, R.A. (1984b) The Bani Ghayy Group Sedimentation and Volcanicity in Pull-apart Graben. *Ministry of Petroleum and Mineral Resources, Deputy Ministry for Mineral Recourses, Jeddah, Kingdom of Saudi Arabia, Open-File-Report DGMR-OF-**05-17***.

Agar, R.A. (1985) Stratigraphy and palaeogeography of the Siham group: Direct evidence for a late Proterozoic continental microplate and active continental margin in the Saudi Arabian Shield, *J. Geol. Soc. London*, **142:** 1205-1220.

Agar, R.A. (1988) Geology of Zalim quadrangle, *Sheet 22f Kingdom of Saudi Arabia Deputy Ministry for Mineral Resourses Map GM 89C.*

Ahmed, H.A., Arai, S. and **Attia, A.** (2001) Petrological characteristics of podiform chromitites and associated peridotites of the Pan African Proterozoic ophiolite complexes of Egypt, *Mineralium Deposita*, **36:** 72-84.

Al Jahdli , N.S. (2004) *Geology of Jabal Ghadara Area, Bir Tawila District with Special Emphasis on Listvenite as a Potential Source for Gold in the Kingdom of Saudi Arabia*, Unpublished M.Sc. Thesis, King Abdulaziz University, Jeddah, Saudi Arabia.

Al-Riyami, K., Robertson, A., Dixon, J. and **Xenophontos, C.** (2002) Origin and emplacement of the late Cretaceous Bear-Bassit ophiolite and its metamorphic sole in NW Syria, *Lithos*, **65:** 225- 260.

Al Shanti, A.M.S. (1993) *Geology of the Arabian Shield*, Scientific Publication Center, King Abdulaziz University, Jeddah Kingdom of Saudi Arabia, 196 p. (In Arabic).

Al Shanti, A.M.S. and **El-Mahdy, O.R.** (2001) *Geology and Tectonic Setting of Ophiolitic Belts in the Arabian Shield*, Saudi Arabia, Mineral Deposits at the Beginning of the 21st Century, Piestrzynski *et al*. (ed.), © 2001 Swets and Zeitlinger Publishers Lisse, ISBN 90 2651 846 3, pp. 631-634.

Al-Saleh, A. and **Boyle, A.P.** (2001) Structural rejuvenation of the Eastern Arabian Shield during continental collision: Ar/Ar evidence from the Ar Ridayniyah ophiolitic mélange, *Journal of African Earth Sciences*, **33** (1): 135- 141.

Azer, M. K. and **Khalil, A.E.S.** (2006) Mineralogy and composition of serpentinites and associated chromitite lenses from Wadi Sodmen area: Implications for magma genesis in a suprasubduction zone, *The 8th International Conference on the Geology of the Arab World (GAW8), Abstracts*, **13**, Cairo, Egypt.

Bakor, A.R., Gass, I.G. and **Neary, C.** (1976) Jabal Al Wask, Northwest Saudi Arabia. An Eocambrian back-arc ophiolite, *Earth and Planet. Science Letters*, **30:** 1-9.

Basta, F.F. (1983) *Geology and Geochemistry of the Ophiolitic Mélange and Other Rock Units in the Area Around and West of Gabal Ghadir, Eastern Desert, Egypt*, Ph. D. Thesis, Cairo Univ., Egypt.

Billa, M. (1987) Exploration of the Jabal Ghadarah gold deposit, Bir Tawilah District, Saudi Arabian *Deputy Ministry for Mineral Resources. Open-File Report BRGM-OF-**06-15**:* 46 p.

Bonavia, F.F., Diella, V. and **Ferrario, A.** (1993) Precambrian podiform chromitites from Kenticha Hill, Southern Ethiopia, *Econ. Geol*., **88:** 198-202.

Brown, G.C. (1979) Calc-alkaline magma genesis: The Pan-African contribution to the crustal growth? In: Al Shanti, A.M.S. (ed.), *Evolution and Mineralization of the Arabian Shield, FES Bull*., **3:** 19-29.

Christensen, N.I. and **Salisbury, M.H.** (1975) Structure and constitution of the lower oceanic crust, *Rev. Geophys. Space. Phys.*, **13:** 57-86.

Church, W.R. (1972) Ophiolite: Its definition, origin as oceanic crust, and mode of emplacement in orogenic belts, with special reference to the Appalachians, *Dep. Energy, Mines Res. Can., Earth Physics, Branch Publ*., **42** (3): 71-85.

Coleman, R.G. (1971) Plate tectonic emplacement of upper mantle peridotite along continental edges, *J. Geophys. Res*., **76:** 1212-1222.

Coleman, R.G. (1977) *Ophiolites, Ancient Oceanic Lithosphere*, Springer-Verlag Berlin, 229 p.

Dewey, J.F. and **Bird, J.M.** (1970) Mountain belts and the new global tectonics, *J. Geophys. Res.*, **75:** 2625-2647.

Dick, H.J.B. and **Bullen, T.** (1984) Chromian spinel as a petrogenetic indicator I abyssal and Alpine-type peridotites and spatially associated lavas, *Contrib. Mineral. Petro*., **86:** 54-67.

Dick, H.J.B. (1977) Partial melting in the Josephine Peridotites I, the effect on mineral composition and its consequence for geobarometry and geothermometry, *Am. J. Sci*., **277:** 801-832.

El Sharkawy, M.A. and **El Bayoumi, R.M.** (1979) The ophiolites of Wadi Ghadir area, Eastern Desert, Egypt, *Ann. Geol. Surv. Egypt*, **IX:** 125-135.

El-Mahdy, O.R. and **Al Shanti, A.M.** (2001) *Geology of Chromite Deposits in the Arabian Shield, Saudi Arabia. Mineral Deposits at the Beginning of the 21st Century*, Piestrzynski *et al.* (eds), © Swets and Zeitlinger Publishers Lisse, ISBN 90 2651 846 3, pp. 607-610.

Elsass, P. and **Vaillant, F.X.** (1983) Geology and mineral exploration of the As Siham-As Suq belt, *Saudi Arabia Deputy Ministry for Mineral Resourses*, Open File Report BRGM-OP-***03-46***.

Evans, B.W. and **Frost, B.R.** (1975) Chrome spinel in progressive metamorphism – a preliminary analysis, *Geochemica Cosmochemica Acta*, **39:** 959 -972.

Feybesse, J.L. and **LeBel, L.** (1984) *Petrographic and Structural Study of the Bir Tawilah Au/W Prospects*, Ministry of Petroleum and Mineral Resources. Directorate General of Mineral Resources Jeddah, Kingdom of Saudi Arabia, Open-File-Report, BRGM-OF-***04-14***.

Fisk, M.R. and **Bence, A.E.** (1980) Experimental crystallization of chrome spinel in FAMOUS basalt 527-1 -1, *Earth Planet. Sci. Lett.*, **48:** 111-123.

Frisch, W. and **Al Shanti, A.** (1977) Ophiolite belts and the collision of island arcs in the Arabian Shield, *Tectonophysics*, **43:** 293-306.

Gansser, A. (1974) The ophiolitic mélange, a world-wide problem on Tethyan examples, *Eclog. Geol. Helv*., **67** (3): 479-507.

Gass, I.G. (1968) Is the Troodos massif of Cyprus a fragment of Mesozoic oceanic floor?, *Nature*, **220:** 39-42.

Gass, I.G. and **Smewing, J.D.** (1981) Ophiolites-obducted oceanic lithosphere, In: Emiliani, C. (Ed.), *The Sea – the Oceanic Lithosphere*, New York (John Wiley and Sons), **7**, pp: 339-362.

Gass, I.G. (1981) Pan-African (Upper Proterozoic) plate tectonics of the Arabian-Nubian Shield, In: Kroner, A. (Ed.) *Precambrian Plate Tectonics*, Amsterdam, Elsevier, pp: 387-405.

Hallberg. (1985) Discrimination Diagrams for Discrimination and Classification of Altered Ancient Volcanic Rocks, In: Richerd, L.R. (Ed.), *Mineralogical and Petrological Data System (**Minpet, version 2.02, copywrite** 1988-1995).*

Harris, R.A. (1987) Structure and composition of subophiolite metamorphic rocks, western Brooks Range ophiolite belt, Alaska, *Geological Society of America Abstracts with Programs*, **19:** 387.

Huot, F., Hebert, R., Varfalvy, V., Beaudoin, G., Wang, C., Liu, Z., Cotton, J. and **Dostal, G.** (2002) The Beimarangg mélange (southern Tibet) brings additional constraints in assessing the origin, metamorphic evolution and obduction processes of the Yarlung Zangob ophiolite, *Journal of Asian Earth Sciences*, **21** (3): 307- 322.

Hutchinson, C.S. (1975) *Ophiolites in Southeast Asia, Geol. Soc. Am. Bull*, **86:** 797-806.

Irvine, T.N. and **Baragar, W.R.A.** (1971) A guide to the chemical classification of the common volcanic rocks, *Canada. J. Earth Sci*., **8:** 523-548.

Irvine, T.N. (1965) Chromian spinel as a petrogenetic indicator; Part 1, Theory, *Can. J. Earth Sci.*, **2:** 648-671.

————. (1967) Chromian spinel as a petrogenetic indicator; Part 2, Petrologic applications, *Can. J. Earth Sci.*, **4:** 71 -103.

————. (1976) Chromite crystallization in the join Mg_2SiO_4 – $CaMgSi_2O_6$ – $CaAl_2Si_2O_6$ – $MgCr_2O_4$, Carnegie Inst. *Wash. Yearbook*, **76:** 465-277.

Johnson, P.R., Kattan, F.H. and **Al Saleh, A.M.** (2003) Neoproterozoic Ophiolites in the Arabian Shield: Field Relations and Structure; *Open - File – Report, SGS - OF -2003 – 1*.

Kemp, J., Pellaton, C. and **Calvez, J.Y.** (1982) *Cycle in the Orogenic Evolution of the Precambrian Shield in Part of Northwestern Saudi Arabian*, Dir. Gen. Miner. Resour. Professional Paper 1, pp: 27-41.

Kroner, A. (1985) Ophiolites and evolution of the tectonic boundaries in the late Proterozoic Arabian-Nubian Shield of Northestern Africa and Arabia, *Precamb. Res*., **27:** 277-300.

Labbé, J.F. (1984) A Preliminary Survey of the Bir Tawilah Gold and Tungsten-tin Prospect, *Open-File-Report BRGM-OF-**04-21***.

Le Maitre, R.W., Bateman, P., Dudek, A., Keller, J., Lameyre, J., LeBas, M.J., Sabine, P.A., Schmid, R., Sorensen, H., Streckeisen, A., Woolley, A.R. and **Zanettin, B.** (1989) Classification of Igneous Rocks and Glossary of Terms, *Blackwell Scientific Publications Oxford, England*, 193 p.

Le Metour, J., Johan, V. and **Tegyey, M.** (1983) Geology of the Ultramafic-Mafic Complexes in the Bir Tuluhah and Jabal Malhijah areas, *Saudi Arabian Deputy Ministry for Mineral Resourses. Open- File Report BRGM- OF- **03- 40***: 47 pp.

Leistel, J.M., Al Jahdali, N., Khalil, I., Kattu, G., Eberle, J.M., Lembert, A., Siddiqui, A. and **Saleh, Y.** (1999) Results of Precious Metal Exploration in the Zalim Prospect, Kingdom of Saudi Arabia, *Saudi Arabian Deputy Ministry for Mineral Resources Technical Report BRGM-TR-**99-14***: 39, p. 108.

Letalenet, J. (1979) Geologic Map of the Afif Quadrangle, sheet 23F, Kingdom of Saudi Arabia, *Saudi Arabian Dir. Gen. Miner. Resour. Geologic Map* **GM-47-A**: 20 p., 1 pl.

Lippard, S.J., Shelton, A.W. and **Gass, I.G.** (1986) The ophiolite of Northern Oman. *Geological Society, London, Memories No.* **11**, 192 p.

Mac Donalds, G.A. and **Katsura, T.** (1964) Chemical composition of Hawaiian lavas, *J. Petrol*., **5:** 82-133.

Miller, B.V. and **Barr., S.M.** (2000) Origin and isotopic composition of a Grenvillian Basement Fragment in the Northern Appalachian Orogen: Blair River Inlier, Nova Scotia, Canada, *Journal of Petrology*, **41:** (12).

Miyashiro, A. (1974) Volcanic rock series in island arc and active continental margins, *American Journal of Science*, **274:** 321-355.

Nassief, M.O., Macdonald, R. and **Gas, I.G.** (1984) The Jabal Thurwah Upper Proterozoic Ophiolite Complex, Western Saudi Arabia, *Journal of the Geological Society, London*, **141:** 537-546.

Paktunc, A.D. (1984) Metamorphism of the ultramafic rocks of the Thompson Mine, Thompson nickel belt, Northern Manitoba, *Canadian Mineralogis*t, **22:** 77-91.

Pearce, J.A. (1975) Basalt geochemistry used to investigate post tectonic enviroment in Cyprus, *Tectonophysics*, **25:** 41-67.

Pearce, J.A. and **Cann, J.R.** (1973) Tectonic setting of basic volcanic rocks determined using trace element analyses, *Earth and Planetary Science Letters*, **19:** 290-300.

Schmidt, D.L., Hadley, D.G. and **Stoeser, D.B.** (1979) Late Proterozoic Crustal History of the Saudi Arabian Shield, Southern Najd Province, Kingdom of Saudi Arabia, In Al Shanti, A. M.S. (Ed.), *Evolution and Mineralization in the Arabian-Nubian Shield*, Volume 2; King Abdulaziz University, *Institute of Applied Geology Bulletin*. 3, Oxford-New York Pergamon Press, pp: 41-58.

Shackleton, R.M., Ries, A.C., Graham, R.H. and **Fitches, W.R.** (1980) Late Precambrian Ophiolitic Mélange in the Eastern Desert of Egypt, *Nature*, **285:** 472-474.

Shervais, J.W. (1982) Ti-V plot and the petrogenesis of modern and ophiolitic lavas, *Earth and Planetary Science Letters*, **59:** 101-118.

Stoeser, D.B. and **Camp, V.E.** (1984) Pan African Microplate Accretion of the Arabian Shield, *Saudi Arabian Deputy Ministry for Mineral Resources. Technical Record USGS-TR-**04-17***.

Takla, M.A. and **Noweir, M.A.** (1980) Mineralogy and mineral chemistry of the ultramafic mass of El-Rubshi, Eastern Desert, Egypt, *N. Jb. Miner. Abh.* **140** (1): 17-28.

Takla, M.A., Hassneinn, Sh. and **Sakran, Sh.** (1990) Geochemistry of the ophiolitic mélange between Idfu-Marsa Alam road and Wadi Shait, Eastern Desert, Egypt, *Egypt. Mineral.*, **2:** 31-50.

Viland, J.G. (1986) *Assessment for Gold in the Zalim area, Central Arabian Shield, Review of BRGM Work*, Ministry of Petroleum and Mineral Resourses, Deputy Ministry for Mineral Resources, Jeddah, KSA, Open File Report BRGM-OF-**O6-11**.

Wernner, G.D. (1987) Saxonian granulites: A contribution to the geochemical diagnosis of the original rocks in high-metamorphic complexes, *Gerlands Beitraege zur geophysik*, **96:** 271-290.

Williams, H. and **Smythe, W.R.** (1973) Metamorphic aureoles beneath ophiolite suites and alpine peridotites, *Tectonic Implication with Western Newfoundland Examples. American Journal of Science*, **273:** 594-621.

Worl, R.G. and **Elsass, F.E.** (1980) *Evolution of Mineralization in Serpentinite and Enclosing Rocks in the Hamdah Area*, Kingdom of Saudi Arabia, U.S Geol. Surv. Saudi Arabian Mission Project Report **276**, 33 p.

جيولوجية وجيوكيميائية الميلانج الأفيوليتي في منطقة جبل غدارة، مربع ظلم، وسط المملكة العربية السعودية

هشام محمد حربي ، و عبدالمنعم عبدالفتاح الدجدج ، و ناصر سعيد الجحدلي*

*كلية علوم الأرض – جامعة الملك عبدالعزيز، و * هيئة المساحة الجيولوجية السعودية*

جـــدة – المملكة العربية السعودية

المستخلص. يمكن تقسيم صخور ما قبل الكامبري الموجودة في منطقة جبل غدارة إلى صخور فوق مافية متحولة، وصخور بركانية رسوبية متحولة (قوسية)، وجرانيتات متزامنة ومتأخرة النشأة التجبلية، ورواسب المولاس، ومونزوجرانيت ما بعد التجبل. وتظهر الصخور فوق المافية المتحولة ويصاحبها انكشاف اللستفينيت على امتداد طول صدع اندفاعي يأخذ اتجاه شمال شمال شرق ويميل باتجاه الشرق، متلامسة مع الصخور البركانية الرسوبية المتحولة. وتتميز الصخور فوق المافية المتحولة بوجود قطع مختلفة الأحجام من الجابرو المتحول، والبازلت المتحول، والشيست، والامفيبوليت، والرخام. ويشير توزيع العناصر الرئيسة والشحيحة إلى أن الجابرو المتحول، والبازلت المتحول، والأمفيبوليت إلى أنها ثولييتية تنتسب إلى قاع المحيط. وقد اشتقت صخور الأمفيبوليت من صخر أولي مافي أو فوق مافي. وأوضح الكروميت الموجود في صخور السربنتنيت واللستفينيت مدى واسع في محتواه من أكاسيد العناصر الرئيسة مشابهًا في ذلك الكروميت من النوع اللألبي. وقد فسر تلازم القطع الصخرية مختلفة الأحجام مع الصخور فوق المافية المتحولة على أنها ميلانج أفيوليتي تراكب مع تتابع الصخور البركانية الرسوبية المتحولة أثناء الحركات التكتونية المصاحبة لعمليات تجبل الدرع العربي مختلفًا في ذلك مع ما أقترح سابقًا بأنها صخور متداخلة.